

Aus der Medizinischen Klinik II

der Universität zu Lübeck

Kommissarischer Direktor: Prof. Dr. J. Weil

**Pentameric C-reactive protein dissociation on microparticles
following myocardial infarction and in the pathogenesis of
Alzheimer's disease.**

Inauguraldissertation

zur

Erlangung der Doktorwürde
der Universität zu Lübeck

- Aus der Sektion Medizin -

vorgelegt von

Frederik Strang

aus Eckernförde

Lübeck 2013

1. Berichterstatter: Prof. Dr. med. Heribert Schunkert
2. Berichterstatter: Priv.-Doz. Dr. med. Dirk Hartwig
3. Berichterstatter: Prof. Dr. med. Jan Torzewski

Tag der mündlichen Prüfung: 18.01.2014

Zum Druck genehmigt: Lübeck, den 18.01.2014

- Promotionskommission der Sektion Medizin -

Table of contents

Table of contents	iii
List of figures	vi
List of tables.....	vii
List of abbreviations.....	viii
1 Introduction	1
1.1 C-reactive protein	1
1.2 Microparticles	3
1.3 Myocardial Infarction	5
1.4 Alzheimer's disease.....	7
1.5 Aims of this thesis	9
2 Materials	10
2.1 Reagents and chemicals	10
2.2 Cell culturing	11
2.3 Blood withdrawal	11
2.4 Equipments and instruments	12
2.5 Antibodies	13
2.6 Immunohistology	13
2.7 Patient samples.....	14
2.8 1,6 bis-phosphocholine.....	15
3 Methods	16
3.1 Cell culturing	16
3.2 Blood withdrawal	16
3.3 Cell stimulation and microparticle isolation	16
3.4 Beta-amyloid plaque growth	17
3.5 Flow cytometry	18
3.5.1 Microparticles in flow cytometry	20
3.6 Polyacrylamide gel electrophoresis (PAGE)	21
3.7 Western blot	22
3.7.1 Microparticle incubation with pentameric C-reactive protein.....	24

3.7.2	Beta-amyloid plaque incubation with pentameric CRP	24
3.7.3	Inhibition of mCRP formation by 1,6 bis-phosphocholine	24
3.8	Monocyte adhesion assay	25
3.9	Aggregometry.....	26
3.9.1	Preparation of platelet rich plasma and platelet poor plasma	27
3.9.2	Aggregometry procedure	27
3.10	Immunohistology	28
3.11	Immunofluorescence staining	30
3.12	Immunohistological analysis	31
3.13	Histological sectioning and processing of the artificial beta-amyloid plaque.....	32
4	Results.....	33
4.1	THP-1 cells, HUVEC and human blood cells	33
4.1.1	THP-1 cells release microparticles under stimulation by LPS.....	33
4.1.2	HUVEC release microparticles under stimulation by TNF- α	33
4.1.3	THP-1- and HUVEC-derived microparticles dissociate pentameric CRP to monomeric CRP.....	34
4.1.4	Whole blood-derived microparticles dissociate pentameric CRP to monomeric CRP which can be inhibited by 1,6 bis-phosphocholine	35
4.2	Monomeric CRP in the context of myocardial infarction.....	37
4.2.1	Monomeric CRP can be detected on circulating microparticles following myocardial infarction	37
4.3	Monomeric CRP in the context of Alzheimer's disease.....	41
4.3.1	Characterization of artificial beta-amyloid plaques	41
4.3.2	Beta-amyloid plaques dissociate pentameric CRP to monomeric CRP	42
4.3.3	Beta-amyloid plaques induce platelet activation.....	44
4.3.4	Beta-amyloid plaques induce monocyte activation.....	45
4.3.5	Monomeric CRP but not pentameric CRP can be detected in brain tissue of patients with Alzheimer's disease.....	46
4.3.6	Monomeric CRP co-localizes with complement component C1q in the cortex of patients with Alzheimer's disease	48
4.3.7	Monomeric CRP co-localizes with beta-amyloid plaques in the cortex of patients with Alzheimer's disease.....	49
5	Discussion.....	51
5.1	Monomeric CRP in the context of myocardial infarction.....	51
5.2	Monomeric CRP in the context of Alzheimer's disease.....	54

5.3	Limitations of this study	58
6	Summary	59
7	Kurzfassung in deutscher Sprache	61
8	References.....	65
9	Acknowledgement	76
10	Curriculum Vita	77
11	Publications.....	78
12	Attachments	79
12.1	Ethics approval for mCRP detection after myocard infarction	79
12.2	Ethics approval for mCRP detection in Alzheimer patient's brain tissue.....	81

List of figures

Figure 1.1 C-reactive protein in its pentameric isoform.	1
Figure 1.2 Micropartilces from Jurkat cells.	3
Figure 2.1 1,6 bis-phosphocholine binding two pentameric CRPs together.....	15
Figure 3.1 Light microscope picture of an artificial beta-amyloid plaque.....	17
Figure 3.2 Basic mechanism of a flow cytometer.	19
Figure 3.3 Identification and classification of microparticles by flow cytometry.....	20
Figure 3.4 Protein separation by polyacrylamide gel electrophoresis.	21
Figure 3.5 Protein staining on a nitrocellulose membrane (Western blot).....	23
Figure 3.6 Preparation of white blood cells from whole blood.....	25
Figure 3.7 The principle of aggregometry.....	27
Figure 3.8 Basic principle of immunohistology.	29
Figure 3.9 Measuring the area of a color in a picture using Image-Pro® software.....	32
Figure 4.1 Antigen expressions of THP-1 cells and THP-1-derived microparticles.	33
Figure 4.2 Antigen expressions of HUVEC and HUVEC-derived microparticles.....	34
Figure 4.3 Microparticles can convert pentameric CRP to monomeric CRP <i>in vitro</i>	35
Figure 4.4 Human blood-derived microparticles can convert pentameric CRP to monomeric CRP <i>in vitro</i>	37
Figure 4.5 mCRP on microparticles detected by Western blot.	40
Figure 4.6 mCRP on microparticles analysed by flow cytometry.....	41
Figure 4.7 Characteristics of artificial beta-amyloid plaques.....	42
Figure 4.7 Beta-amyloid plaque induced dissociation of pentameric to monomeric CRP.	43
Figure 4.8 Histological proof of monomeric CRP generation by an artificial beta-amyloid plaque.....	44
Figure 4.9 Beta-amyloid plaques activate platelets as shown by aggregometry.....	45
Figure 4.10 Beta-amlyoid plaques induce monocyte activation.	46
Figure 4.9 Identification of mCRP but not pCRP in human brain tissue from Alzheimer's disease patients with beta-amyloid plaques.	47
Figure 4.10 Statistical analysis of the stained area in patients with and without Alzheimer's disease.	48
Figure 4.11 Monomeric CRP and C1q co-localization.	49
Figure 4.12 Monomeric CRP and beta-amyloid plaques co-localization.....	50
Figure 5.1 The possible role of CRP in the development of Alzheimer's disease.	57

List of tables

Table 2.1 Alzheimer’s disease patient’s characteristics.....15

Table 3.1 Characteristics of the fluorochromes used in this thesis.31

Table 4.1 Clinical and demographic characteristics of STEMI and PCI control groups.....39

List of abbreviations

ADP	adenosine diphosphate
APP	amyloid precursor protein
APS	ammonium persulfate
Aβ	beta-amyloid
Aβ₄₂	beta-amyloid peptide fragment with 42 amino acids
BBB	blood-brain barrier
bisPC	1,6 bis-phosphocholine
BSA	bovine serum albumin
Ca	Calcium
CAD	coronary artery disease
CCP	classical complement pathway
CK	creatine kinase
CRP	C-reactive protein
DAB	3,3'-diaminobenzidine-tetrachloride
DES	drug eluting stent
FACS	fluorescence activated cell sorting
FCS	fetal calf serum
FSC	forward scatter
FITC	fluorescein isothiocyanate
HCL	hydrochloric acid
HRP	horse radish peroxidase
hrs	Hours
HUVEC	human umbilical vein endothelial cells
LPS	Lipopolysaccharide
MAC	membrane attack complex
mCRP	monomeric C-reactive protein
Mg	Magnesium
min	Minutes
NEAA	non-essential amino acids
nm	Nanometres
OD	optical density
P	Probability
PAGE	polyacrylamide gel electrophoresis

PBS	phosphate buffered saline
PC	phosphocholine
PCI	percutaneous intervention
pCRP	pentameric C-reactive protein
PE	R-Phycoerythrin
PMA	phorbol 12-myristate 13-acetate
PPP	platelet poor plasma
PRP	platelet rich plasma
PS	phosphatidylserine
RPM	rounds per minute
RT	room temperature
SDS	sodium dodecyl sulfate
sec	seconds
SEM	standard error of the mean
SSC	side scatter
STEMI	ST elevation myocardial infarction
TEMED	N, N, N', N'-tetramethylethylenediamine
TNF-α	tumor necrosis factor α
VBBN	Victoria Brain Bank Network

1 Introduction

1.1 C-reactive protein

C-reactive protein (CRP) was first identified in 1929 after being isolated due to its ability to precipitate the C polysaccharide of streptococcus (1). It was this property which gave the protein its name. Over 50 years later, in 1983, Whitehead *et al.* discovered the gene locus of CRP on chromosome 1 (2) paving the way for recent genome studies investigating the association of high CRP levels and an increased risk of coronary heart disease (3).

The prototypic acute phase reactant, CRP is a member of the pentraxin family of proteins and is highly conserved among a wide variety of species (4). It is predominantly synthesised in the liver in response to inflammatory stimuli, particularly interleukin-6 (1), interleukin-1 and tumor necrosis factor α (TNF- α). This response is very rapid (within 6 hours) and can dramatically increase serum CRP levels. It is this property that underlies CRP's utility as a marker of inflammation. CRP circulates as a disc shaped pentamer (figure 1.1) consisting of five identical non-covalently bound 23 kDa subunits (1) each with a length of 206 amino acids. It has two functional faces, a phosphocholine binding site and an effector face.

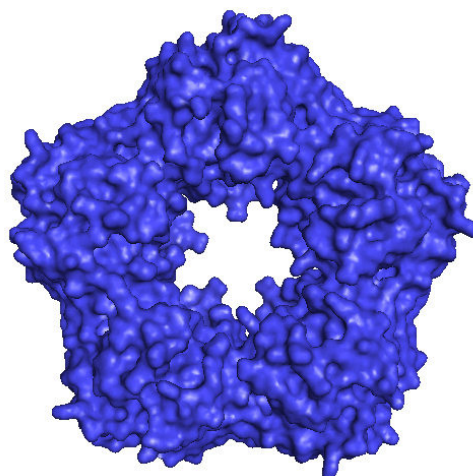


Figure 1.1 C-reactive protein in its pentameric isoform.

The picture shows the C-reactive protein as it circulates in the human blood stream after response to inflammatory stimuli. The five subunits are forming a disc shaped pentamer around a central pore. (Picture was generated with information from the RCSB Protein Data Bank by using PyMOL software).

In a wide range of inflammatory diseases CRP appears to play a role or at least act as a biological bystander. CRP has a long association with cardiovascular disease as an increase in circulating CRP was recognised as a common clinical finding in patients following myocardial infarction (5). Further studies have demonstrated a consistent correlation between CRP elevation and a variety of adverse outcomes following myocardial infarction including left ventricular failure (6) and death (7-8). More recently it has been recognised that chronic, minor elevations of CRP are associated with the development of cardiovascular disease independent of the traditional Framingham risk criteria (9). It has been shown in an elegant animal model of myocardial infarction that CRP leads to a complement mediated increase in infarct size (10). CRP levels are also lower at sites of plaque rupture when compared to the general circulation (11), supporting a direct pathological role for CRP in myocardial infarction. This finding is in agreement with observational clinical data (12).

In Alzheimer's disease, the most common form of irreversible dementia, inflammation appears to play a major role in the pathogenesis (13-15) even though the pathomechanism is not fully understood at present. Given these facts it is not surprising that level of the CRP are increased (16) and co-localization of CRP with senile plaques has been shown in brain sections from patients with Alzheimer's disease (17). Although elevated levels of CRP are associated with Alzheimer's disease the direct link between CRP and Alzheimer's disease pathophysiology is still not known.

CRP recognises a wide variety of endogenous and exogenous ligands in its function as part of the innate immune system (18). Following ligand engagement, CRP can directly activate the complement cascade and Fc receptors to promote phagocytosis. Given these properties and the observational clinical data, it was widely expected that CRP would play a direct pathogenic role in inflammation and atherosclerosis. However, circulating pentameric CRP (pCRP) does not appear to interact significantly with complement or the regulatory complement Factor H (19). Studies of CRP in chronic inflammation using a variety of methods including animal models (20), meta-analyses (21) and Mendelian randomisation studies (22) have been unable to establish a direct pathogenic role for CRP (23). Therefore there is an unresolved conflict in the current CRP data; it appears to be a marker rather than a causal factor correlated with the development of atherosclerosis,

driven by low grade chronic inflammation. However, in acute inflammation such as that found after myocardial infarction it seems to directly mediate tissue damage. An elegant solution to this dichotomy might be the dissociation of pCRP to its monomeric isoform. It has been shown that following binding to a variety of lipid surfaces including activated cell membranes (24) and liposomes (25) pCRP undergoes dissociation to individual monomers (mCRP). mCRP has distinct pro-inflammatory properties not shared with pCRP including C1q fixation (25), platelet activation (26) and monocyte chemotaxis (24). This raises the possibility that (m)CRP may contribute directly to the pathogenesis of infarct size following myocardial infarction, Alzheimer's disease and other inflammatory associated diseases. This hypothesis is supported by the previous identification of mCRP in atherosclerotic plaques (24).

1.2 Microparticles

In 1967 Wolf *et al.* described platelet-derived microparticles as “cellular dust” (27) for the first time. Microparticles are sub-micrometre (figure 1.2) vesicles with a range of $\sim 0.1 - 1 \mu\text{m}$ (28) derived from cell membranes. Particles smaller than 100 nm, formally known as exosomes, differ from microparticles not only in size but also in their configuration and synthesis (29).

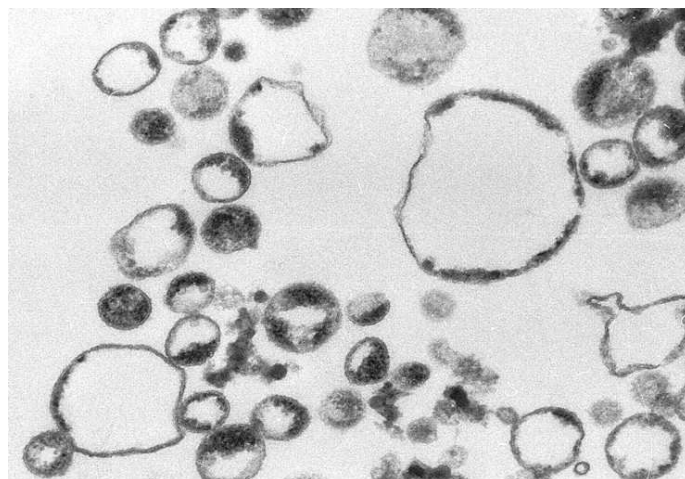


Figure 1.2 Micropartilces from Jurkat cells.

This picture shows the ultrastructure of microparticles shed from Jurkat cells by transmission electron microscopy. The vesicle range from 200 nm to 700 nm. Magnification 80,000x. (Picture from Distler *et al.* (2004) The induction of matrix metalloproteinase and cytokine expression in synovial fibroblasts stimulated with immune cell microparticles. *Proc Natl Acad Sci U S A* 102: 2892-2897)

Microparticles are present in the circulation of both healthy and diseased subjects; however levels are elevated in a wide variety of inflammatory disease states including malignancy (30), atherosclerotic vascular disease (31), rheumatoid synoviocytes (32) or simply inflammation (33-34). They consist of phospholipids and proteins derived from their parent cell and have been shown to promote a variety of biological processes including inflammation, thrombosis and angiogenesis (35). In healthy subjects microparticles have physiological functions in intercellular communication, haemostasis, and immunity (28).

The exact synthesis and release mechanism of microparticles is not fully understood yet. But different groups showed a key role of increased cytosolic calcium (Ca) concentration (36-38) after activation or apoptosis. These studies showed the inhibition of microparticle formation by using a Ca^{2+} chelating compound such as ethylene glycol-bis(beta-aminoethyl ether)-N,N,N',N'-tetraacetic acid (EGTA). A variety of agonists such as lipopolysaccharide (LPS) or $\text{TNF-}\alpha$ activate monocytes and endothelial cells, respectively (32, 39); whereas platelets get activated by thrombin and collagen. The activation causes Ca^{2+} release from the intracellular Ca^{2+} stores and an enhanced Ca^{2+} influx, causing an increase in the cytosolic Ca^{2+} concentration which leads to cytoskeleton degeneration due to calcium-dependent proteolysis (40-41). The higher Ca^{2+} concentration may also lead to lipid scramblase and floppase activation. Both enzymes stabilize the asymmetric bilayer membrane and maintain the specific lipid composition of the inner and outer leaflet (42). Both mechanisms contribute to the loss of membrane asymmetry and cytoskeleton degeneration which induces vesiculation and microparticle release.

Due to the loss of the asymmetry of the cell membrane the outer leaflet of the microparticles membrane expresses the negatively charged lipid phosphatidylserine (PS), which is typically found on the inner membrane surface of cells (43). *In vitro* studies have shown that the negatively charged surface has the capacity to bind coagulation factors and mediate coagulation (44-47).

Microparticles reflect the protein content such as receptors and antigens of their parent cell. These antigens are detectable with different methods like flow cytometry and characteristic antigens enable an assignment of microparticles to their cell of origin.

As a wide variety of diseases are associated with elevated microparticle levels as mentioned above it is noteworthy that some disorders are associated with decreased microparticles levels. A bleeding disorder with isolated prolonged bleeding time and a deficiency of platelet microparticle generation (48) highlights the importance of microparticles in normal haemostasis. Interestingly, patients with acute myocardial infarction have a low total microparticle count (49) which is consistent with our findings.

1.3 Myocardial Infarction

Myocardial infarction remains one of the leading causes of death in industrial countries. The World Health Organisation estimated that 12.8 % of all deaths worldwide in 2008 were due to ischemic heart disease (50). In Germany alone nearly 65,000 patients died of myocardial infarction and its sequelae in 2004.

During an acute myocardial infarction the blood supply to the heart muscle provided by the coronary arteries is interrupted or decreased causing hypoxia. After a sufficient period of time the resulting ischemia results in damage and death to the heart muscle cells.

The underlying pathomechanism for an interruption of normal blood flow is coronary artery disease (CAD) which can be caused by a variety of conditions including atherosclerosis, thrombosis, coronary spasm, embolisms, extra luminal coronary artery restriction, decreased perfusion pressure, decreased diastolic pressure, increased central venous pressure or decreased diastolic time period. The most common form of CAD is atherosclerosis. Vulnerable atherosclerotic plaques are a result of advanced atherosclerosis. They are a collection of lipids, white blood cells (mostly macrophages) and other proteins in the arterial wall and are covered with a thin fibrous cap. The mechanism behind the formation of vulnerable and stable plaques is not fully understood at present and is the subject of intensive current research. The main risk is a rupture of a vulnerable plaque which can result in a thrombosis of the following artery with the above mentioned consequences. Several risk factors were identified over the last couple of years. The most important risk factors are:

- Dyslipidemia (51)
- Smoking (51)

- High blood pressure (51)
- Diabetes (52)
- High age and male gender (53)
- Obesity (54)
- Genetic predisposition (53)

CRP is also recognised as an independent risk factor since Paul Ridker published an remarkable and highly discussed paper in the New England Journal in 2002 (55).

The diagnosis of an acute myocardial infarction has 3 major components, the symptoms the patient presents with, ECG changes and cardiac biomarkers like troponin and creatine kinase - MB fraction. According to the World Health Organisation (WHO) the diagnosis of acute myocardial infarction requires an elevation in cardiac troponin accompanied by either typical symptoms, pathological Q waves, ST elevation or depression, or coronary intervention (56).

As most European countries can provide an emergency health system in which a patient presenting with an acute myocardial infarction can be in the catheterisation laboratory within 90 minutes (min) the gold standard therapy for an acute myocardial infarction is percutaneous coronary intervention (PCI). During this procedure the cardiologist uses either the femoral artery, the radial artery or the brachial artery to gain access to the coronary arteries. A catheter is used to inject contrast medium into the coronary arteries which can then be imaged through real-time x-ray. This procedure enables the cardiologist to estimate the localization and size of the stenosis and artery. With this information the cardiologist will select the right balloon catheter and coronary guide wire. As a next step the guiding wire with a radio-opaque flexible tip will be placed to the site of the stenosis or blockage. Once the guide wire is in place the balloon catheter will be placed over the guide wire. The balloon catheter is then inflated and the plaque is compressed into the wall of the artery. In the majority of cases an expandable wire mesh tube (stent) is placed around the balloon and will now keep the re-opened artery open and stabilize it from the inside. Today there are two different types of stents available. The traditional bare metal stents simply stabilize the vessel wall after the balloon inflation and the newer drug eluting stents (DES) which are coated in immunosuppressive drugs loaded on a polymer construct. The DES will release

the drugs over time and will prevent re-stenosis of the artery by suppressing growth factors, inflammation and immune responses.

In countries such as Australia where a catheter laboratory is not always reachable within 90 min fibrinolysis therapy is recommended. The maximum effect will be seen when thrombolysis is performed within 1-3 hours (hrs). Current thrombolytic drugs in clinical use include streptokinase, alteplase and reteplase.

To prevent a recurrent myocardial infarction the progression of the CAD will be treated with acetylsalicylic acid (e.g. Asperin®) and/or Clopidogrel, a β -blocker, a statin and an ACE-inhibitor.

1.4 Alzheimer's disease

Alzheimer's disease is the most common form of irreversible dementia (57). It was first described by Alois Alzheimer in 1907 (58) when he reported of a 51 year old patient with cerebral atrophy and neuronal changes he had only seen in the elderly until then. Over a century later Alzheimer's disease has become one of the most disabling and burdensome health conditions worldwide (59). Today, we can distinguish a hereditary familial from the sporadic form of Alzheimer's disease. The hereditary form occurs only in 5% of patients but appears much earlier in life than the sporadic form. Even though the exact pathomechanism remains elusive, over the past decades genes which cause beta-amyloid ($A\beta$) overproduction have been identified as risk factors for developing hereditary Alzheimer's (60). The inheritance of the $\epsilon 4$ allele of apolipoprotein E is known as one of the major genetic risk factors (61-63) and leads to an extensive deposition of $A\beta$ in the cerebral cortex (64). For the more frequent sporadic form several hypotheses exist trying to explain the cause of Alzheimer's disease. There is the $A\beta$ hypothesis which states that $A\beta$ deposition is the essential cause of the disease (65). Then there is the tau hypothesis postulating hyperphosphorylated tau protein as the initial cause of Alzheimer's disease (66). Hyperphosphorylated tau forms neurofibrillary tangles inside nerve cell bodies leading to microtubule disintegration and the neuron's transport system collapses (67). A third, but less supported hypothesis, implicates reduced synthesis of the neurotransmitter acetylcholine as a basis for Alzheimer's disease. The lack of support for this hypothesis is mainly because medications that have been used to treat acetylcholine deficiency have not been very effective in clinical practice. Nevertheless, in both forms of

Alzheimer's disease our understanding of the pathological process central to the progression of Alzheimer's disease is incomplete.

The current therapeutic agents available to clinicians serve predominantly to modify patient symptoms and are unable to halt the progressive decline in cognitive function that is the hallmark of Alzheimer's disease (68). As one of the main changes in patients with Alzheimer's disease is the reduced synthesis of the neurotransmitter acetylcholine, cholinesterase inhibitors are used as first line therapy. The three cholinesterase inhibitors permitted for use in Alzheimer's disease in Germany are Donepezil, Galantamin and Rivastigmin. In more advanced disease the NMDA receptor antagonist Memantin is also permitted as later on the glutamatergic systems is dysfunctional as well. It is hoped that new generations of agents will be able to slow or even halt the progression of dementia. However, it is likely that any significant therapeutic advance will rely upon an improvement in our current understanding of the pathophysiology of Alzheimer's disease, enabling novel treatment approaches to be developed.

As stated previously there is extensive data which strongly supports the central role of A β in the pathogenesis of Alzheimer's disease (65). The A β peptide is cleaved from the transmembrane amyloid precursor protein (APP) by β - and γ -secretases. Normally, the APP is cleaved by α - and γ -secretases leading to the soluble APPs- α , p3 and CT fragments. In Alzheimer's disease the most important A β peptide fragment is an insoluble 42 amino acid peptide (A β_{42}). A β_{42} peptides aggregate and are the dominant component of the diffuse senile plaques (69) found in the brain tissue of Alzheimer's disease patients.

Senile plaque formation initiates the inflammatory processes, which are responsible for neuronal cell death leading to the progression of Alzheimer's disease. Consistent with this understanding, increased levels of the pro-inflammatory cytokine interleukin-6 have been found in the brains of Alzheimer's disease patients (16). Further supporting data has documented complement and microglial activation (70), along with increased numbers of reactive astrocytes (71). The level of the acute phase reactant CRP is also increased (16) and co-localization of CRP with senile plaques has been shown in brain sections from Alzheimer's disease patients (17). Although elevated levels of CRP are associated with Alzheimer's disease there is currently no direct evidence linking CRP to the pathophysiology of Alzheimer's disease.

1.5 Aims of this thesis

The aim of this thesis was to identify whether microparticles have the capacity to dissociate pCRP to mCRP *in vitro* and if mCRP can be found on microparticles following myocardial infarction *in vivo*.

As a second goal the capacity of A β plaques to dissociate pCRP to mCRP was assessed *in vitro*. The clinical relevance of this dissociation process was evaluated by measuring the mCRP burden in the frontal cortex of patients with and without Alzheimer's disease.

2 Materials

2.1 Reagents and chemicals

Item	Company
Acrylamid 40%	Amresco®
Adenosine diphosphate (ADP)	Sigma
Agarose	Promega
Ammonium persulfate (APS)	Sigma
BD Cellfix™	BD Biosciences
Beta Amyloid Peptide (1-42)	Genscript
Bovine serum albumin (BSA)	Sigma
Ethanol	Biolab (Aust.) Ltd.
Fibronogen	Sigma
Gelantine	Sigma
Hydrochloric acid (HCL)	Sigma
LPS	Sigma
Recombinant mCRP	Gift from Larry Potempa
Methanol	Biolab (Aust.) Ltd.
NaAC	Sigma
Phosphate buffered saline (PBS)	Media Service Baker IDI Melbourne
PBS with Ca ²⁺ /Mg	Media Service Baker IDI Melbourne
pCRP	Calbiochem®
Phosphatase substrate	Sigma
Phorbol 12-myristate 13-acetate (PMA)	Sigma
Precision Plus Protein™	Bio-Rad
SuperSignal® West Pico Chemiluminescent	Thermo Scientific
N, N, N', N'-tetramethylethylenediamine (TEMED)	Sigma
TNF-α	Sigma
Triton® X-100	Sigma
Trizma® base, minimum	Sigma
Tween® 20	Sigma

2.2 Cell culturing

Item	Company
THP-1 Cells	ATTC™
175cm ² cell culture flask	BD Biosciences
6-well cell culture plate	BD Biosciences
75cm ² cell culture flask	BD Biosciences
EBM®-2	Lonza
EGM® -2 SingleQuots®	Lonza
Fetal calf serum (FCS)	Invitrogen™
Gelatine	s. reagents
Human umbilical vein endothelial cells (HUVEC)	ATTC™
L-Glutamin	Invitrogen™
Non essential amino acids (NEAA)	Invitrogen™
Penicillin	Invitrogen™
RPMI 1640	Invitrogen™
Streptomycin	Invitrogen™
Trypsin-EDTA	Invitrogen™

2.3 Blood withdrawal

Item	Company
BD Vacutainer®	BD Biosciences
Monovette® 10.0 ml	Sarstedt
Monovette® 2.9 ml	Sarstedt
Muli-Adapter	Sarstedt

2.4 Equipments and instruments

Item	Company
Aggregometer AggRAM™	Helena Laboratories
Alegra™ 21 Centrifuge	Beckmann Coulter
BD FACSCanto™ II Flow Cytometer	BD Biosciences
BD Falcon™ 15ml	BD Biosciences
BD Falcon™ 50ml	BD Biosciences
Beads 0.8um	BD Biosciences
Beads 1.1um	BD Biosciences
Film Developer	AGFA
Electrophoresis Glass Plates	Bio-Rad
Eppendorf Centrifuge 5415D	Eppendorf AG
Eppendorf Centrifuge 5810	Eppendorf AG
Eppendorf tube 0,6 ml	Eppendorf AG
Eppendorf tube 1.5 ml	Eppendorf AG
Eppendorf tube 2.0 ml	Eppendorf AG
Ficoll-Paque™ Plus	GE Healthcare
GraphPad Prism® v5.0	GraphPad Software, Inc.
High performance chemiluminescence film	GE Healthcare
Horizontal Rotator	Hoefer
Image-Pro® plus v6.0	Media-Cybernetics, Inc.
Immobilon™ Transfer membrane	Millipore™
Incubator Hepa Class 100	Thermo Scientific
Lightmicroscope BX50	Olympus
Lightmicroscope CKX41	Olympus
Lightmicroscope FSX-100	Olympus
Maxisorp 96 wells plate	nunc™
Microplate Manager® 6 software	Bio-Rad
Mini-PROTEAN 2-D Cell	Bio-Rad
PyMOL	Schrödinger®
Wet/Tank Blotting Systems	Bio-Rad
xMark™ Microplate Absorbance Spectrophotometer	Bio-Rad

2.5 Antibodies

Item	Company
Anti-human CD 106 PE conjugated	BD Pharmingen
Anti-human CD 11b FITC conjugated	Beckmann Coulter
Anti-human CD 14 FITC conjugated	Beckmann Coulter
Anti-human CD 144 PE conjugated	R+D Szstems
Anti-human CD 18 FITC conjugated	Beckmann Coulter
Anti-human CD 31 FITC conjugated	BD Pharmingen
Anti-human CD 41 PE conjugated	Beckmann Coulter
Anti-human CD 45 PE conjugated	BD Pharmingen
Anti-human CD 54 FITC conjugated	Chemicon International
Anti-human CD 62P PE conjugated	BD Pharmingen
Goat anti-mouse FITC conjugated	Millipore™
Goat anti-mouse HRP conjugated	Millipore™
Mouse anti-human mCRP (clone 3H12)	Gift from Larry Potempa
Mouse anti-human mCRP (clone 8C10)	Gift from Larry Potempa
Mouse anti-human mCRP (clone 9C9)	Gift from Larry Potempa
Mouse anti-human pCRP (clone 1D6)	Gift from Larry Potempa
Mouse anti-human pCRP (clone 8D8)	Gift from Larry Potempa
Mouse IgA Isotype Control FITC	Beckmann Coulter
Mouse IgA Isotype Control PE	Beckmann Coulter
Rabbit anti-human C1q (H-55)	Santa Cruz Biotechnology Inc.
Goat anti-rabbit Alexa Fluor 488 conjugated	Invitrogen™
Goat anti-mouse Alexa Fluor 555 conjugated	Cell Signaling Technology

2.6 Immunohistology

Item	Company
Avidin/Biotin Blocking Kit	Vector Laboratories
DAB Peroxidase Substrate Kit	Vector Laboratories
VECSTAIN ABC Kit	Vector Laboratories
VECSTAIN Elite ABC Kit	Vector Laboratories

2.7 Patient samples

Patient samples for studying mCRP on microparticles after myocardial infarction were recruited as followed: The patient population was divided into two groups. Patients who presented with a ST elevation myocardial infarction (STEMI) on ECG and underwent primary PCI were defined as the STEMI group. The second group acted as a PCI control group; these patients underwent PCI for a non-emergent indication. Patients were recruited 24 to 48 hrs post PCI as this is typically when serum CRP peaks enabling the greatest sensitivity in detecting mCRP.

Patients with any of the following criteria were excluded; age >80, thrombolysis during admission, intra-aortic balloon pump insertion, sepsis (defined as positive blood culture during admission), haemorrhage requiring transfusion or creatinine clearance <60ml/min as estimated by the Cockcroft-Gault formula.

All patient recruitment was performed following approval from the relevant institutional human ethics committee and all patients gave informed consent before enrolment.

Patients samples for studying mCRP in Alzheimer's disease were obtained from the Victorian Brain Bank Network (VBBN), supported by The University of Melbourne, The Mental Health Research Institute of Victoria, Alfred Hospital and the Victorian Forensic Institute of Medicine and funded by Australia's National Health and Medical Research Council, The Helen Macpherson Smith Trust, Parkinson's Victoria and Perpetual Philanthropic Services.

Human brain tissue from 7 patients diagnosed with Alzheimer's disease and 7 non-Alzheimer's disease cases as controls were analysed (for patient's characteristics see table 2.1). The VBBN provided 6 μ m thick formalin fixed and paraffin embedded sections from the frontal cortex.

One non- Alzheimer's disease case was excluded because of typical senile plaque pattern seen in the A β (NAB228) staining.

Health studies were approved by local research ethics committees, and all individuals gave informed consent.

	AD cases	Non AD controls	P value	Summary
age	80.69 (74.6-88.4)	78.25 (72.6-82.7)	P > 0.05	ns
PMI (h)	42.57	42.00	P > 0.05	ns
Cases (female/male)	7 (4/3)	6 (2/4)	P > 0.05	ns
CVD	0.29	0.67	P > 0.05	ns

Table 2.1 Alzheimer's disease patient's characteristics.

The Alzheimer patients and the patients selected as control group show no significant differences in age, sex and the presence of cardiovascular diseases. AD = Alzheimer's disease, PMI = post mortem interval, CVD = cardiovascular diseases

2.8 1,6 bis-phosphocholine

1,6 bis-phosphocholine (bisPC) was purchased from Syngene International, India. BisPC is a specific pCRP inhibitor which acts to combine two pCRP (figure 2.1) molecules preventing membrane binding. BisPC function was assessed using a phosphorylcholine agarose affinity column.

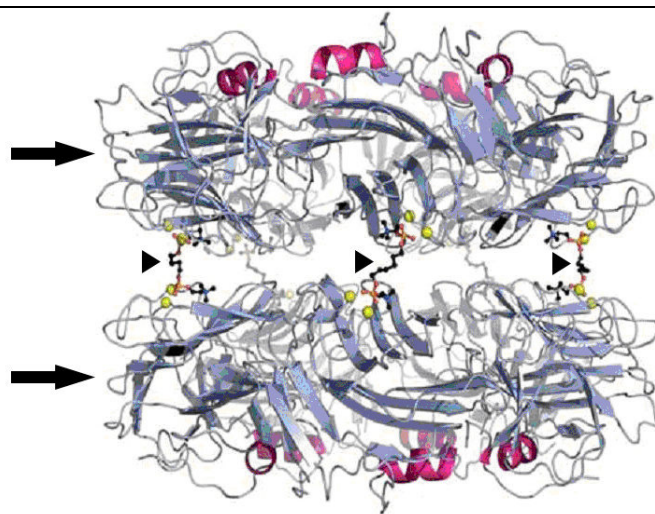


Figure 2.1 1,6 bis-phosphocholine binding two pentameric CRPs together.

The picture shows five bisPC (arrow heads) binding two pCRPs together (arrows). (Picture from Pepys MB et al. (2006) Targeting C-reactive protein for the treatment of cardiovascular disease. Nature.440(7088):1217-21)

3 Methods

3.1 Cell culturing

THP-1 cells were kept in RPMI 1640 medium with 10% FCS, 1% streptomycin, 1% Penicillin, 1% L-glutamine and 1% NEAA in 175cm² cell culture flasks in an incubator at 37° C with 5% CO₂. Cells were split every second to third day to a number of 2x10⁵ cells per ml.

HUVEC were kept in EBM®-2 medium with EGM® -2 SingleQuots® in 6-well cell culture plate in an incubator at 37° C with 5% CO₂. The 6-well plate was pre-incubated for 1 h at 37° C with 0.1% gelatine and washed twice afterwards with phosphate buffered saline (PBS) before cells were added. Medium was changed every two days until cells were dense (approx. 166 x 10³ cells/well) and used for experiments. All experiments were performed between passage 3 and 6.

3.2 Blood withdrawal

Venous blood from patients or healthy volunteers was taken with a 21-gauge BD Vacutainer® from the cubital vein using a tourniquet and collected in a 10 ml Monovette® citrate tube. The skin was disinfected with ethanol before the vein was punctured.

3.3 Cell stimulation and microparticle isolation

THP-1-derived microparticles were obtained with slight modification of the method previously published (32). Briefly, cultured THP-1 cells were treated with 15 µg/ml LPS for 18 hrs. The cell suspension was then centrifuged for 15 min at 1,000 x g after an initial spin of 5 min at 400 x g at room temperature (RT). The cell free supernatant was harvested and centrifuged for 90 min at 16,100 x g at 4° C. The pellet was resuspended in 500 µl PBS with Ca (0.90 mM) and magnesium (0.49 mM) (Ca/Mg) and kept on ice until usage.

HUVEC-derived microparticles were obtained with minor adaptation of the protocol described previously (39). HUVEC were stimulated with 100 ng/ml TNF-α for 24 hrs. The supernatant of each well, containing approximately 166x10³ cells, was taken and dead cells and cell fragments were separated by centrifugation for 10 min at 1,000 x g. The cell free supernatant was harvested and centrifuged for 60

min at 16,100 x g at 4° C. The pellet was resuspended in 500 µl PBS with Ca/Mg and kept on ice until usage.

Venous blood from patients was taken with a 21-gauge BD Vacutainer® and collected in a 10 ml Monovette® citrate tube. Patient's blood samples were then centrifuged for 15 min at 1,500 x g at RT and the platelet poor plasma (PPP) was collected. Microparticles were then stained with antibodies for flow cytometry analysis. For polyacrylamide gel electrophoresis (PAGE) patient's microparticles were pelleted with an additional centrifugation step at 16,100 x g for 60 min. at 4° C.

3.4 Beta-amyloid plaque growth

A β_{42} was dissolved in 100% methanol and aliquots were frozen at -20° C until used. To grow A β plaques *in vitro* a slightly different method to that described elsewhere (72) was performed. Briefly, 55 µM (final concentration) of A β_{42} were added to PBS with 0.9 mM Ca (to avoid self-dissociation described previously (73)) and 0.49 mM Mg in a polypropylene tube. The tube was placed on a horizontal rotator at ~ 1Hz and plaque formation was visible after 24 to 48 hrs (figure 3.1).

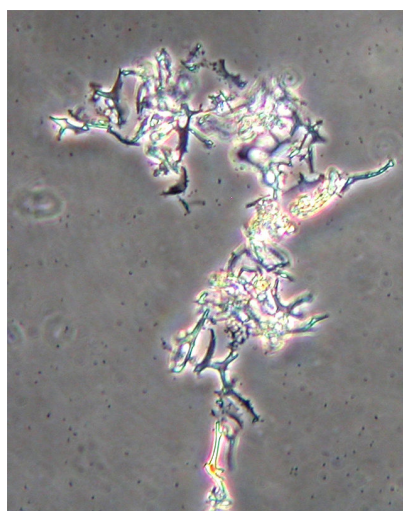


Figure 3.1 Light microscope picture of an artificial beta-amyloid plaque.

The picture shows the structure of an artificial beta-amyloid plaque as seen under the light microscope (magnification 40x).

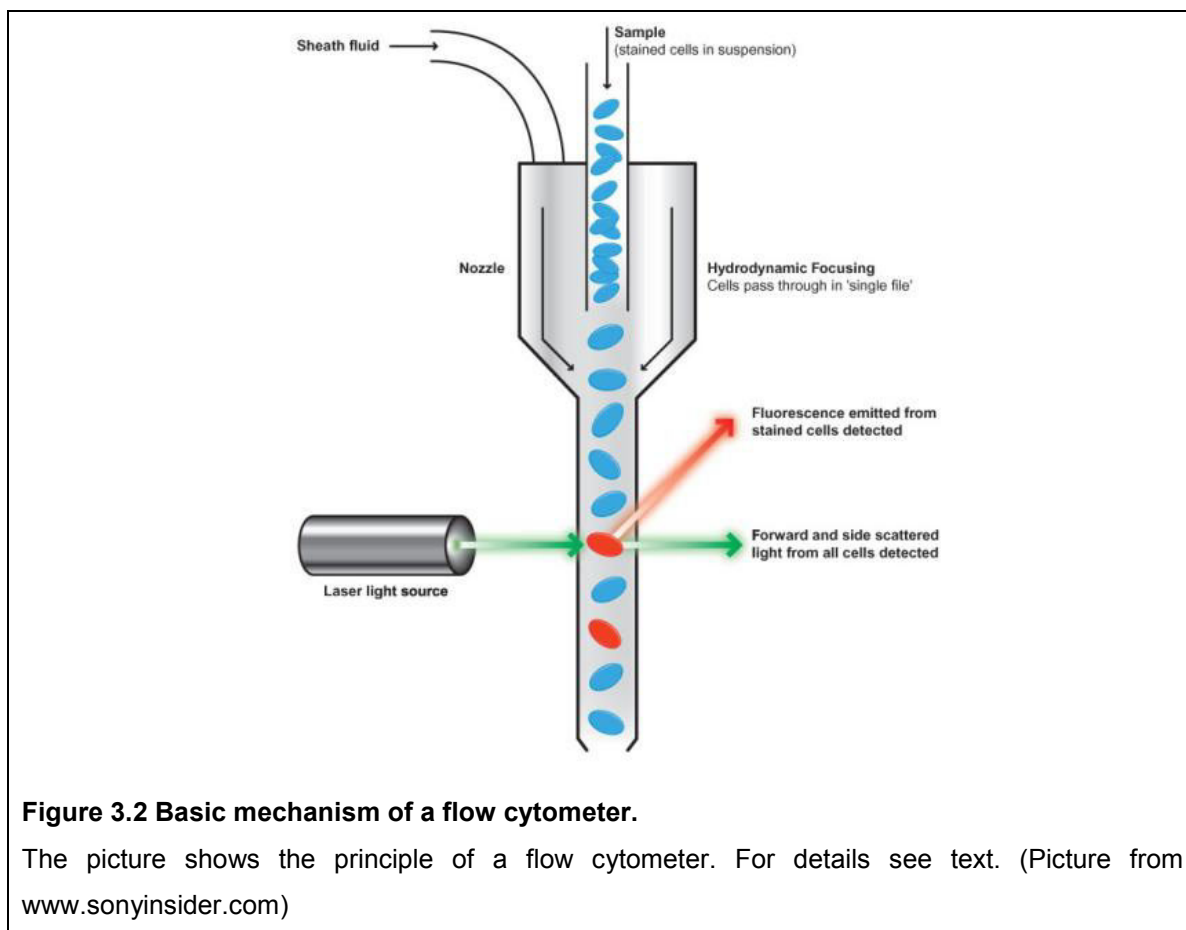
For the immunohistology 275 µM (final concentration) of A β_{42} were added to PBS with Ca/Mg in a polypropylene tube and placed on a horizontal rotator at ~ 1 Hz for

24 to 48 hrs. The supernatant was removed and the plaque was fixed in low melting agarose (Sigma, USA) in the tube. After the agarose set the agarose with plaque was removed from the tube, placed in OCT Compound for cryostat sectioning Tissue-Tek® (Sakura, Netherlands) and frozen at - 80° C.

3.5 Flow cytometry

Flow cytometry or Fluorescence activated cell sorting (FACS) is an optical technique used mainly in clinical practice and research to count and characterize different particles like cells or microparticles by their antigen expression, volume and inner complexity.

The samples need to be in suspension and were prepared as mentioned under 3.3 (Cell activation and microparticles isolation). For analyses the test specimen are directed into a hydrodynamically-focused stream of fluid. A beam of light (in these experiments the flow cytometer projected a laser beam) of a single wavelength is focused at a right angle onto the stream of fluid. Different detectors are placed around the point where the beam of light intersects the stream. One detector is in line with the beam known as the forward scatter (FSC) and measures the ray scatter in an angle of 0-10°. The grade of scatter depends on the cross sectional area which gives information about the volume of the particle passing the laser. Several perpendicular detectors known as side scatter (SSC) provide information about the inner complexity of the particle passing the laser. A third type of detectors measures the fluorescence of the particle (figure 3.2).



Fluorescence is the emission of light by the fluorochrome that has absorbed the laser light previously. The fluorochrome absorbs energy of a specific wavelength (called excitation) and re-emits energy at a different wavelength specific to the individual fluorochrome. The re-emitted energy, the fluorescence, is measured by the fluorescence detector. The flow cytometer used in these experiments has 3 lasers with the wavelengths 405 nm, 488 nm and 633 nm. In the present thesis only 2 fluorochromes were used:

- PE (R-**P**hycoerythrin) with 3 excitation peaks at 480, 546 and 565nm and an emission maximum at 475 nm.
- FITC (**F**luorescein **i**sothiocyanate) with excitation at 492nm and an emission peak at 519nm.

All information collected by the detectors is processed by a computer to visualize the data. Each recognized event counted by the detectors is placed as a dot in a dot blot diagram. Usually, one axis of the dot blot diagram is assigned to the FSC and the other one to the SSC. In this way the particles are sorted by volume and inner complexity. Particles of similar volume and similar inner complexity are

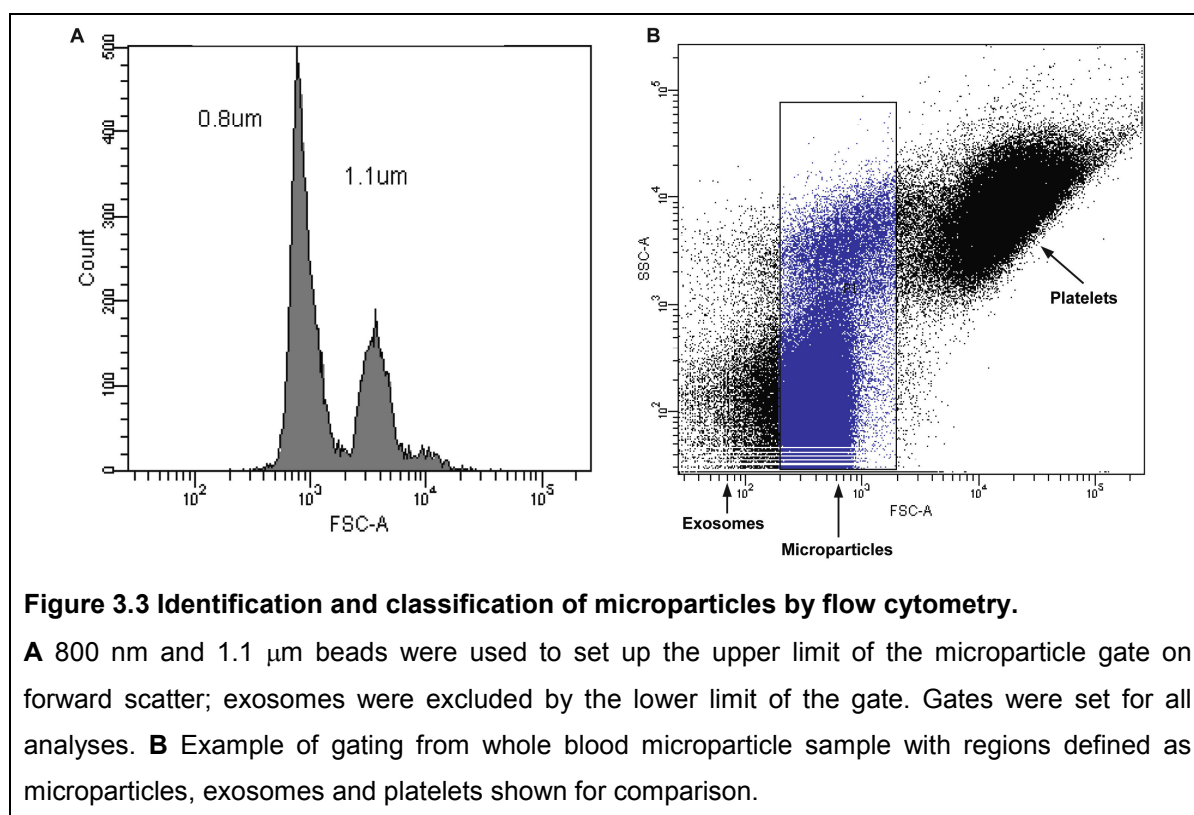
placed in the same area allowing the observer to set a gate isolating the population of interest. Now only the particles in the gate will be analysed.

After the population of interest has been identified the expression of an antigen can be visualized by using a fluorochrome conjugated antibody. In a histogram the frequency distribution of a specific fluorescence is displayed. The mean fluorescence or the percentage of the particles with a specific fluorescence intensity can be derived from that histogram.

In the present study a FACS Canto II flow cytometer and FACS Diva software were used to perform all experiments involving flow cytometry.

3.5.1 Microparticles in flow cytometry

To set up the upper gate limit for the microparticle gate 0.8 μm and 1.1 μm beads were used as described previously (74) and a lower gate limit was set to avoid the smallest particles formally known as exosomes (figure 3.3).



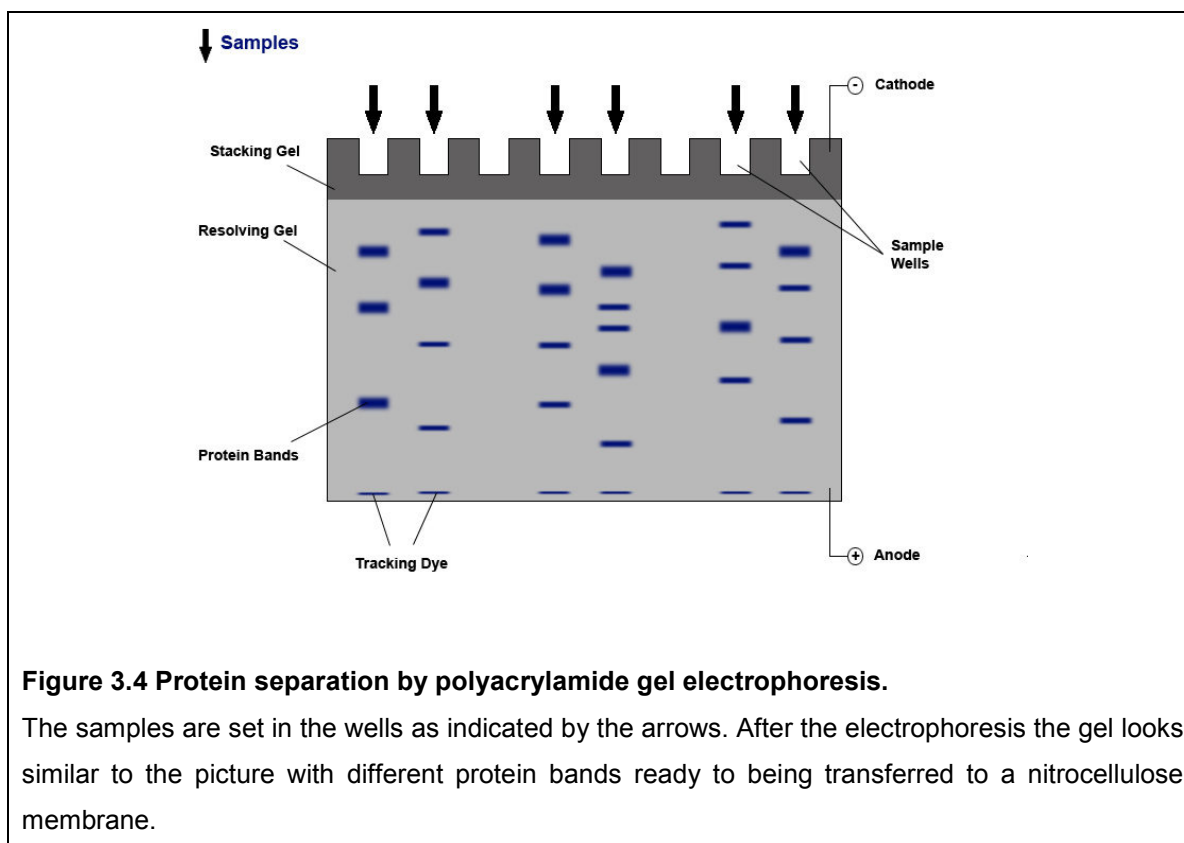
THP-1-derived microparticles were stained with antibodies against CD 11b, CD 18 or CD 45 for 20 min. HUVEC-derived microparticles were stained with antibodies against CD 106, CD 31, CD 54 or CD 14 for 20 min. All reactions were performed

at RT in a dark container. For fixation 500 µl CellFix™ were added to the specimen. All samples were then stored in the dark at 4° C until analysis within 6 hrs.

To count HUVEC-derived, THP-derived or total patient's microparticles; samples with microparticles were diluted 1:10 and counted at medium flow rate for 30 seconds. With $MP_t = Ev / t * FR * DF$ (MP_t = total microparticles; Ev = events; t = time [30 sec]; FR = flow rate [medium on Canto II = 60 µl / 60 sec]; DF = dilution factor [10]) total microparticles / µl were calculated.

3.6 Polyacrylamide gel electrophoresis (PAGE)

The PAGE is a method to separate proteins based on their charge and molecular weight (figure 3.4).



The most common PAGE is the sodium dodecyl sulphate (SDS) PAGE where proteins are denatured by SDS and heating to 95° C. As CRP will not stay in its pentameric isoform through these two denaturing steps it is necessary to use a PAGE without SDS or heating to avoid pentameric to monomeric CRP conversion. This technique is referred to as native PAGE. In both the native and SDS PAGEs,

the percentage stated applies to the amount of acrylamide. The higher the concentration of acrylamide the smaller the pore size of the gel and the slower the running speed of proteins with a high molecular weight.

The following amounts are required to produce a 10% gel of a size of 8.6 cm x 6.8 cm x 1.5 mm.

For native PAGE the resolving gel was made out of 7.50 ml H₂O, 3.75 ml 1.5M Tris HCL pH 8.8, 3.75 ml 40 % acrylamide, 75 µl APS and 15 µl TEMED and was poured between two glass plates fixed by the manufacturer's holding equipment. For a smooth upper surface a small layer of distilled water was added to the top of the gel between the glass plates.

After 30 min the water was removed and the stacking gel was poured on top of the set resolving gel. To prepare the stacking gel 2.15 ml H₂O, 0.83 ml 1.5M Tris HCL pH 6.8, 0.325 ml 40 % acrylamide, 25 µl APS and 5 µl TEMED were used. At last a comb to form 10 wells was placed in the stacking gel.

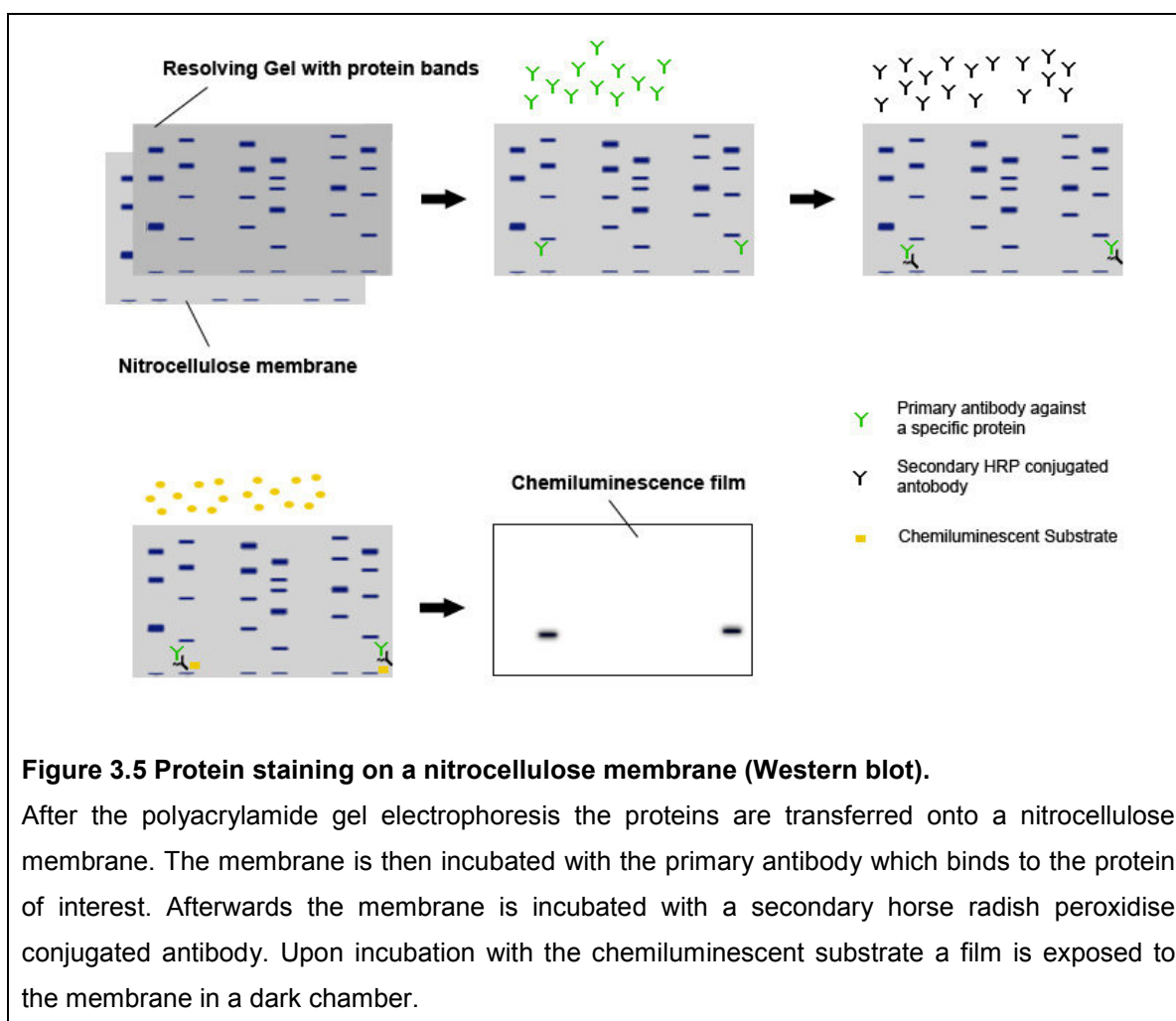
The gel was placed in its holder which was then placed in the tank and native running buffer was added to the tank. 10 times running buffer was made out of 144 gm glycine and 30.2 gm Trizma® base, minimum.

Before the samples could be added the comb was removed gently. If not specified otherwise 25 µl of sample was added to 8 µl of non-reducing native loading buffer and finally 25 µl of this solution was added to the well.

The lid was set on tank and connected to the power supply. The voltage was set at a constant value of 60 V for 30 min. After that the voltage was increased to 120 V for another 60 min, approximately.

3.7 Western blot

In a Western blot the proteins fixed in the resolving gel of the aforementioned PAGE are transferred to a nitrocellulose membrane for staining for specific antigens (figure 3.5).



Again a special non-reducing transfer buffer without SDS is necessary for a native Western Blot as described previously (24). The transfer buffer was made out of 200 ml methanol, 800 ml ddH₂O, 2.9 g glycine and 5.8 g Trizma® base, minimum. The gel with the proteins was surrounded by the nitrocellulose membrane on one side and 2 filter papers and 2 sponges on each side and fixed in the manufacture's holding equipment. The transfer was performed at 4° C overnight at 30 V.

The membrane was blocked the next day with PBS with 0.2 % with Tween® 20 and 1 % BSA for 90 min. Afterwards the primary antibody (clone 9C9 or 8D8) was diluted 1:250 in the aforementioned blocking solution and incubated with the membrane for 2 hrs. Before the secondary antibody was added the membrane was washed four times with PBS with 0.2% Tween® 20 for 20 min. The secondary antibody (HRP conjugated goat anti mouse) was diluted 1:5000 in the blocking solution and incubated with the membrane for 60 min. Unbound secondary antibody was washed off by four washing steps with PBS with 0.2 % Tween® 20 for 20 min. Finally the membrane was incubated with SuperSignal West Pico

Chemiluminescent substrate as per the manufacture's manual and exposed to a film for 30 to 90 sec in a dark room. The film was immediately developed in a developing machine.

3.7.1 Microparticle incubation with pentameric C-reactive protein

To evaluate the dissociation of pCRP to mCRP by Western blot aliquots of isolated HUVEC-, THP-1- and human blood-derived microparticles were isolated as indicated previously and then incubated with pCRP at a final concentration of 20 $\mu\text{g/ml}$ for 60 min at 37° C. Non-reducing loading buffer was added to the samples before they were run on a native PAGE and blotted onto a nitrocellulose membrane as described above. Membranes were stained with antibody clones 8D8 (pCRP specific) or 9C9 (mCRP specific).

3.7.2 Beta-amyloid plaque incubation with pentameric CRP

To evaluate the dissociation of pCRP to mCRP by Western blot an artificial plaque (55 μM), non-aggregated peptide (55 μM) or PBS with Ca and Mg were incubated with pCRP (Merck) at a final concentration of 20 $\mu\text{g/ml}$ for 60 min at 37° C. Non-reducing loading buffer was added to samples before they were run under native PAGE conditions and blotted onto a nitrocellulose membrane as described above. Membranes were stained with antibody clones 8D8 (pCRP specific) or 9C9 (mCRP specific).

3.7.3 Inhibition of mCRP formation by 1,6 bis-phosphocholine

Citrated whole blood was collected from healthy volunteers and stimulated with 20 μM ADP for 20 min. Whole blood was spun at 1,500 x g for 15 min. The top two thirds of plasma were collected and any remaining cells were pelleted by a further 2 minute spin at 13,000 x g. Concentrated microparticles were then prepared by centrifugation at 30,000 x g for 90 min. After centrifugation a microparticle depleted plasma sample was collected from the top of the preparation and the remainder carefully discarded. The concentrated microparticle preparation was then resuspended in 100uL of PBS with Ca and Mg for experimental use.

The microparticle and control preparations were incubated with either pCRP (25 $\mu\text{g/ml}$) alone or pCRP with bisPC. Incubation was performed with pCRP : bisPC

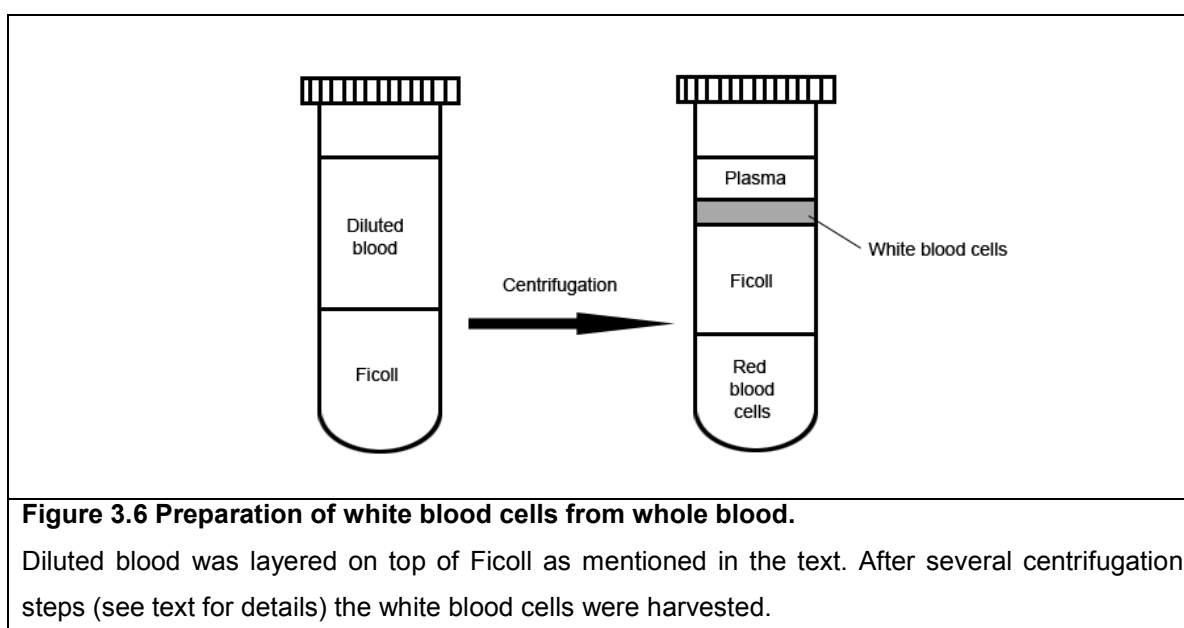
molar ratios as shown. All incubation steps were performed for 60 min at 37° C. Samples were run on a native PAGE and blotted as described below. The membrane was stained with the specific mCRP antibody clone 9C9.

3.8 Monocyte adhesion assay

To analyse the monocyte activation the following monocyte adhesion assay was established.

A Maxisorp® 96-well plate was coated with 20 µg/ml fibrinogen in PBS with Ca and Mg overnight at 4° C. The next day the wells were washed twice with PBS and blocked with 0.1 % agarose for 60 min at RT. Next, the wells were washed twice with PBS and 2×10^5 purified monocytes per well were added. Monocytes were purified as following:

60 ml citrated venous blood from healthy volunteers was diluted 1:2 with PBS. 20 ml of the dilution were added on top of 15 ml Ficoll® and centrifuged for 20 min at 160 x g at RT without using a brake. The top 10 ml were discarded before the blood was spun a second time at 350 x g for 20 min at RT again without using a brake. The mononuclear cells were harvested (figure 3.6) and diluted in washing buffer (= cold PBS with 2 mM EDTA and 0.1 % BSA). To pellet the cells the suspension was spun at 400 x g for 15 min at RT. Afterwards the pellet was resuspended in cold PBS and counted to adjust the cells to two million monocytes per ml after the last spin at 230 x g for 10 min at RT.



Different reagents (see results for details) were added to the wells in triplets and stored in an incubator for 30 min at 37° C to let the monocytes adhere. PMA as a positive control was added after 15 min at a final concentration of 20 nM. Afterwards the wells were washed several times with PBS to remove non-adherent cells and were then incubated with 100 µl of substrate (= 6.54 ml NaAc [50 mM] pH 5 with 66 µ Triton X100 and 40 mg phosphatase substrate) for 60 min at 37° C. At last the reaction was stopped with 50 µl 1 M NaOH and the optical density (OD) was measured at 405 nm in a microplate reader.

3.9 Aggregometry

Once platelets are activated they start to aggregate as a physiological reaction by a positive feedback loop. Aggregometry is a technique to evaluate the aggregation and thus the function of platelets but also to characterize different agonists.

The agonist (in most experiments ADP) will lead to a conformational change of the surface receptor GPIIb/IIIa on the platelets. The activated receptor will bind fibrinogen and hence will cross link the platelets. *In vivo* the agonists are extracellular matrix components such as collagen, ADP or thrombin. Another use for aggregometry is the evaluation of therapeutic drugs such as the ADP blocker clopidogrel or antibodies against the GPIIb/IIIa receptor like Abciximab.

There are two different methods available:

1. impedance aggregometry first described by Cardinal (1979) for the assessment of platelet function in whole blood
2. light transmittance aggregometry (LTA, „Born-Aggregation“, 1963) for the assessment of platelet function in platelet rich plasma (PRP)

In this thesis only light transmittance aggregometry was used. In this method the light transmittance is measured over a certain time period (in the present study 10 min). When the agonist initiates the aggregation of the platelets the number of free platelets decreases and the light transmittance increases (figure 3.7) which is recorded by the detectors.

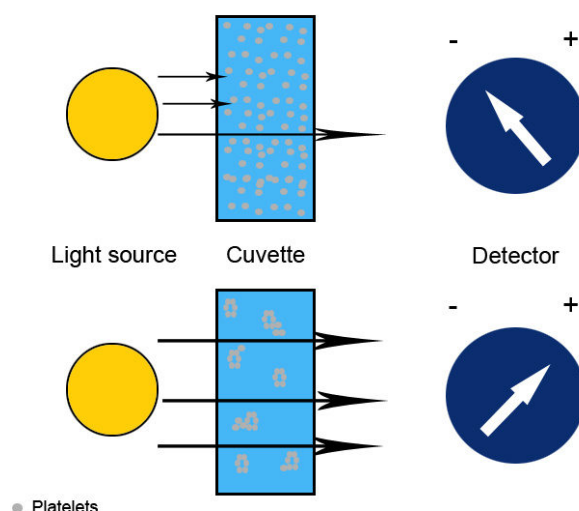


Figure 3.7 The principle of aggregometry.

With more free platelets in the plasma the light transmittance is relatively low (upper picture). When an agonist induces the aggregation of the platelets (lower picture) the optical density decreases which leads to a higher light transmittance. The detectors record the change in light transmittance over time.

As PPP has almost no platelets the optical density is very low and the light transmittance very high. Therefore, the light transmittance of PPP is set as 100 % aggregation.

To see if a reagent can enhance the aggregation triggered by an agonist like ADP the reagent can be pre-incubated with the PRP.

3.9.1 Preparation of platelet rich plasma and platelet poor plasma

To obtain PRP 10 ml blood was taken from healthy volunteers as mentioned above. To avoid platelet aggregation due to this procedure the blood was taken slowly and carefully.

The blood was spun at 1,000 rounds per minute (RPM) for 10 min in an Eppendorf Centrifuge 5810 with reduced brakes. The top 2 ml were collected and the rest was spun a second time for 10 min at 3,000 RPM in the same centrifuge to obtain PPP. PPP was used to calibrate the value for 100 %.

3.9.2 Aggregometry procedure

The AggRAM™ aggregometer was warmed up while the PPP and PRP were prepared. All channels were calibrated with 250 µl PPP to set the highest possible

light transmittance as 100% aggregation. All cuvettes were equipped with a magnetic stirrer. The cuvettes were then filled with 175 μ l of PRP and pre-incubated for 15 min with 50 μ l of either pCRP (diluted), A β plaques or PBS as a negative control (for final concentrations s. results) at 37° C. Afterwards, 25 μ l of 10 μ M ADP were added to induce the aggregations process. The change of light transmittance was recorded for 10 min from that point.

3.10 Immunohistology

Immunohistology is a technique to visualize proteins, antigens, cells or any other component in tissue sections. In the following experiments the DAB technique was used. Basically, the sections are incubated with a primary antibody against a specific protein. Afterwards, the sections are incubated with a biotinylated secondary antibody against the primary before the sections are incubated with an avidin / biontinlyated enzyme complex. As a last step the sections are incubated with the enzyme substrate (in the following experiments 3,3'-diaminobenzidine-tetrachloride (DAB)) which will color the section in the area where the primary antibody bound the antigen of interest (figure 3.8).

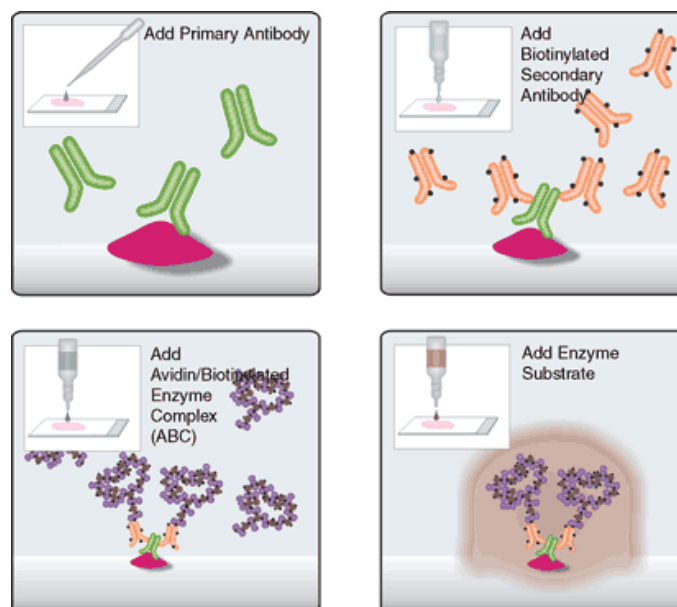


Figure 3.8 Basic principle of immunohistology.

The picture shows the basic steps of immunohistology. After incubation with the primary antibody, secondary antibody and the avidin/biotinylated enzyme complex the enzyme substrate stains the areas where the primary antibody bound the antigen. (Picture from www.vectorlabs.com)

Staining was performed as described previously (75) with some modification. The sections were de-paraffinized and rehydrated in a rack using the following steps:

1. Xylene: 2 x 3 min
2. Xylene 1:1 with 100% ethanol: 3 min
3. 100% ethanol: 2 x 3 min
4. 95% ethanol: 3 min
5. 70 % ethanol: 3 min
6. 50 % ethanol: 3 min
7. Running cold tap water to rinse

Afterwards the sections were boiled for 10 min in concentrated citric acid pH 6.0 as described before (76). The sodium buffer solution was obtained according to the following protocol:

- Tri-sodium citrate (dihydrate) 2.94 g
- Distilled water 1000 ml
- Mix to dissolve. Adjust pH to 6.0 with 1N HCl.
- Add 0.5 ml of Tween 20 and mix well. Stored at room temperature for 3 months or at 4°C for longer storage.

Upon antigen retrieval the sections were treated with 0.5 % H_2O_2 in methanol for 30 min and then blocked with 10 % normal rabbit serum in PBS for 30 min. Primary antibodies were diluted in 2 % normal rabbit serum with 0.3 % triton X-100 in PBS, added to the slides and incubated overnight at 4° C. Biotinylated anti-mouse secondary antibody (diluted 1:1000 in 2% normal rabbit serum in PBS) was added for 1 h before addition of the tertiary antibody (ABC Vectastain Elite kit, Vector) for 1 h. The slides were incubated with the DAB substrate chromogen solution for 10 min and then counter stained with haematoxylin and eosin for 30 seconds (sec). Finally, sections were dehydrated with 100% ethanol, cleared in xylene and covered with DePeX® and cover slipped.

3.11 Immunofluorescence staining

The principle of immunofluorescence staining is very similar to immunohistology. The great advantage of immunofluorescence is that double staining allows the scientist to determine whether two antigens are co-localized.

Instead of a biotinylated secondary antibody against the primary antibody a fluorochrome labelled secondary antibody is used in the indirect immunofluorescence. To analyse two different antigens the two primary antibodies have to be from two different species so that the secondary fluorochrome labelled antibodies will only recognize one antigen indirectly. The two secondary antibodies need to be labelled with two different fluorochromes which will re-emit light at two different wavelengths upon two different excitations. The 3 fluorochromes used in this thesis are found in table 3.1.

Name	Color [#]	Ex (nm)	Em (nm)
Alexa Flour 488	green	495	519
Alexa Flour 555	red	555	565
Thioflavin T	green	485	550

Table 3.1 Characteristics of the fluorochromes used in this thesis.

The usage of different fluorochrome allows the detection of two or more antigens in one specimen as each fluorochrome will emit light in its typical spectrum. Ex (nm) = Excitation wavelength in nanometres, Em (nm) = Emission wavelength in nanometers, [#] = approximate color of the emission spectrum

For the co-localization assays in this thesis, sections from the human frontal cortex were de-paraffinized, rehydrated and incubated in 0.1% CaCl₂ at 50° C overnight and then blocked with 10 % BSA for 30 min. Primary antibodies were diluted in 1 % BSA added to the slides and incubated overnight at 4° C. The fluorochrome labelled anti-mouse and anti-rabbit secondary antibodies (diluted in 1% BSA) were added for 2 h in the dark at RT. Thioflavin T staining was performed with 3 mM freshly filtered aqueous thioflavin T solution for 10 min at RT, which was followed by 2 washing steps in 80% ethanol and 1 washing step in 95% ethanol with subsequent washing in distilled water. Finally, sections were mounted with Aquatex® mounting media and covered with a cover slip. Pictures were taken on an Olympus IX81 microscope at 60x magnification. Microscope settings were obtained with single fluorescence stained sections and controls in which primary antibodies had been omitted.

3.12 Immunohistological analysis

The immunohistological staining in Alzheimer's disease patients was quantified in each slide by measuring the DAB positive tissue of 7 different areas of the cortex with Image-Pro® (figure 3.9); 2 slides per patient were analysed. An average of all 14 pictures per patient and antibody was used for statistical tests.

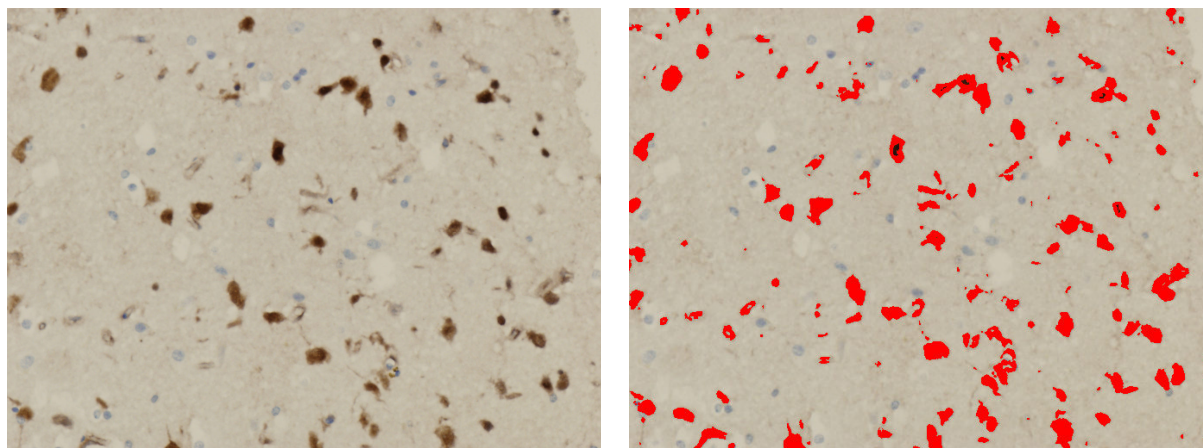


Figure 3.9 Measuring the area of a color in a picture using Image-Pro® software.

The raw picture as taken from the microscope is seen on the left hand side. The staining (brown colour) was assessed by using Image-Pro® and the area of the positive stained tissue was measured (indicated as red in the right picture).

3.13 Histological sectioning and processing of the artificial beta-amyloid plaque

The artificial plaque fixed in agarose as mentioned under 3.4 was cut on a CM 3000 cryosection system (Leica) into 6 μm sections and stained with the ABC Vectastain kit (Vector) (76). Sections were thawed for 30 min before being fixed in acetone at -20°C for 20 min, incubated in 3% v/v H_2O_2 in methanol for 10 min, blocked with 10 % normal rabbit serum (Vector), followed by avidin and biotin blocking for 20 min. The slides were incubated with primary antibody clones 8D8, 9C9 or NAB228 at 4°C overnight. Sections were then incubated with a biotinylated anti-mouse secondary antibody (diluted 1:1000) for 30 min prior to incubation with the tertiary antibody for 30 min. Afterwards the slides were incubated with DAB substrate chromogen solution for 5 min. Sections were finally dehydrated with 100% ethanol, cleared in xylene and mounted with DePeX® (Sigma).

For thioflavin T staining slides were blocked with 10% normal rabbit serum and then incubated with freshly filtered 3mM aqueous thioflavin T solution for 8 min followed by washing in 2 changes of 80% ethanol for 2 min and one change of 95% ethanol for 1 min. After subsequent washing with 3 exchanges of distilled water slides were mounted in Aquatex® mounting media (Merck).

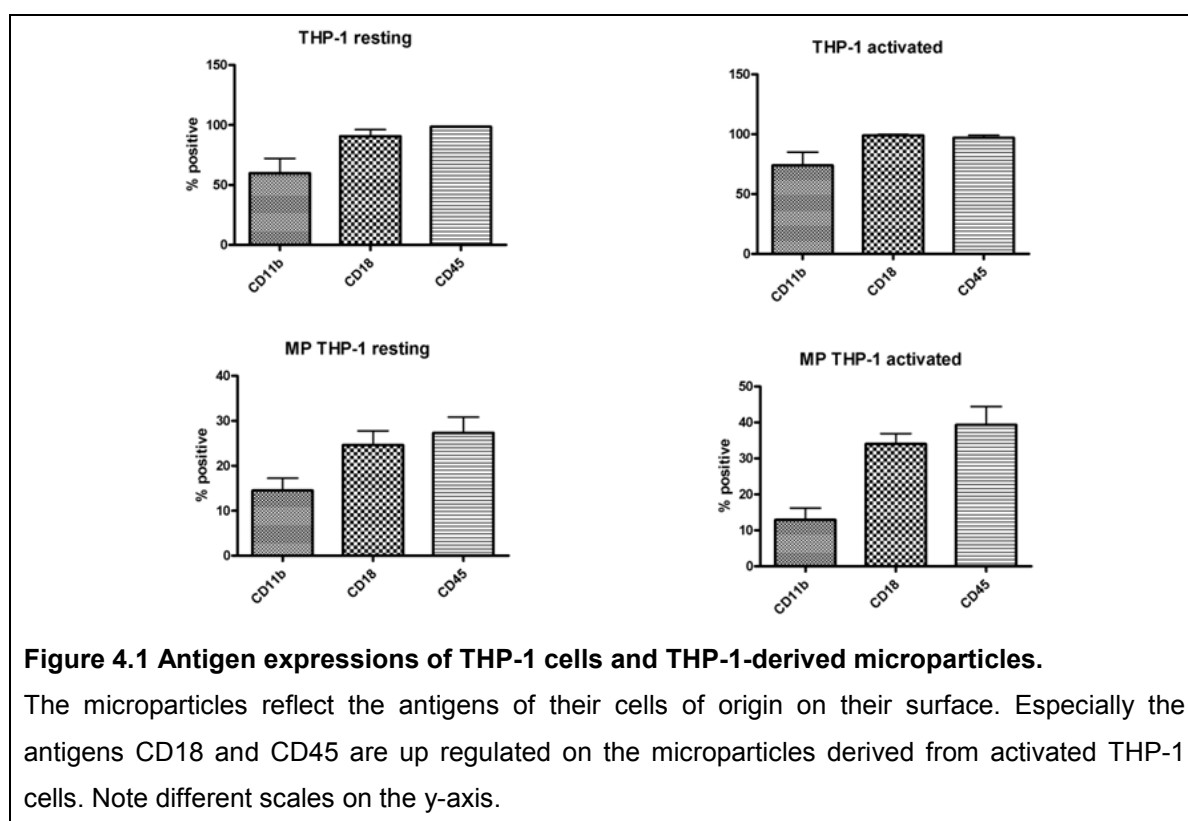
4 Results

4.1 THP-1 cells, HUVEC and human blood cells

4.1.1 THP-1 cells release microparticles under stimulation by LPS

THP-1 cells were stimulated with 15 µg/ml LPS over 18 hrs and microparticles were isolated as described in the methods section. The activated cells and isolated microparticles were then used to investigate their antigen expression pattern in order to compare them to the antigen expression pattern of resting THP-1 cells and microparticles derived from resting THP-1 cells.

The cellular surface markers in the microparticle population were assessed by flow cytometry in order to validate the machine settings and confirm changes in cellular activation. In both cases the markers expressed on the surface of microparticles reflected their cell type of origin (figure 4.1).

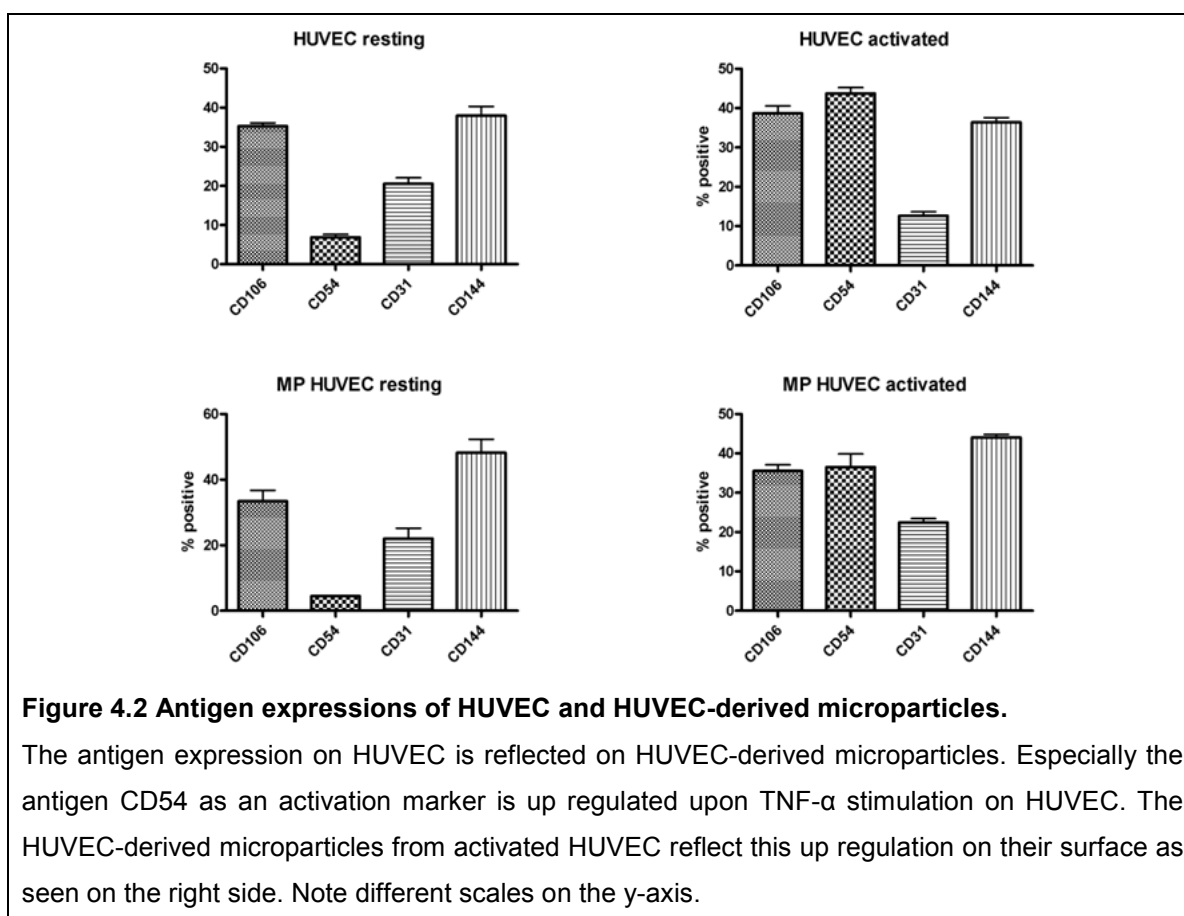


4.1.2 HUVEC release microparticles under stimulation by TNF-α

HUVEC stimulated with 100 ng/ml TNF-α for 24 hrs and the microparticles were isolated as described above. Afterwards, the antigen expression pattern of

stimulated cells, resting cells, microparticles derived from activated cells and resting cells were established using flow cytometry as described above.

The antigen expression pattern of THP-1 cell microparticles reflected that seen in the parent cells. A similar observation was seen in the antigen expression pattern of the resting cells and microparticles derived from them (figure 4.2). Of particular note, the up regulation of the antigen CD54 as (recognised as an activation marker for HUVEC (77)) seen on the activated cells was reflected in the microparticles derived from the activated cells supporting the hypothesis that these microparticles were released from the HUVEC.

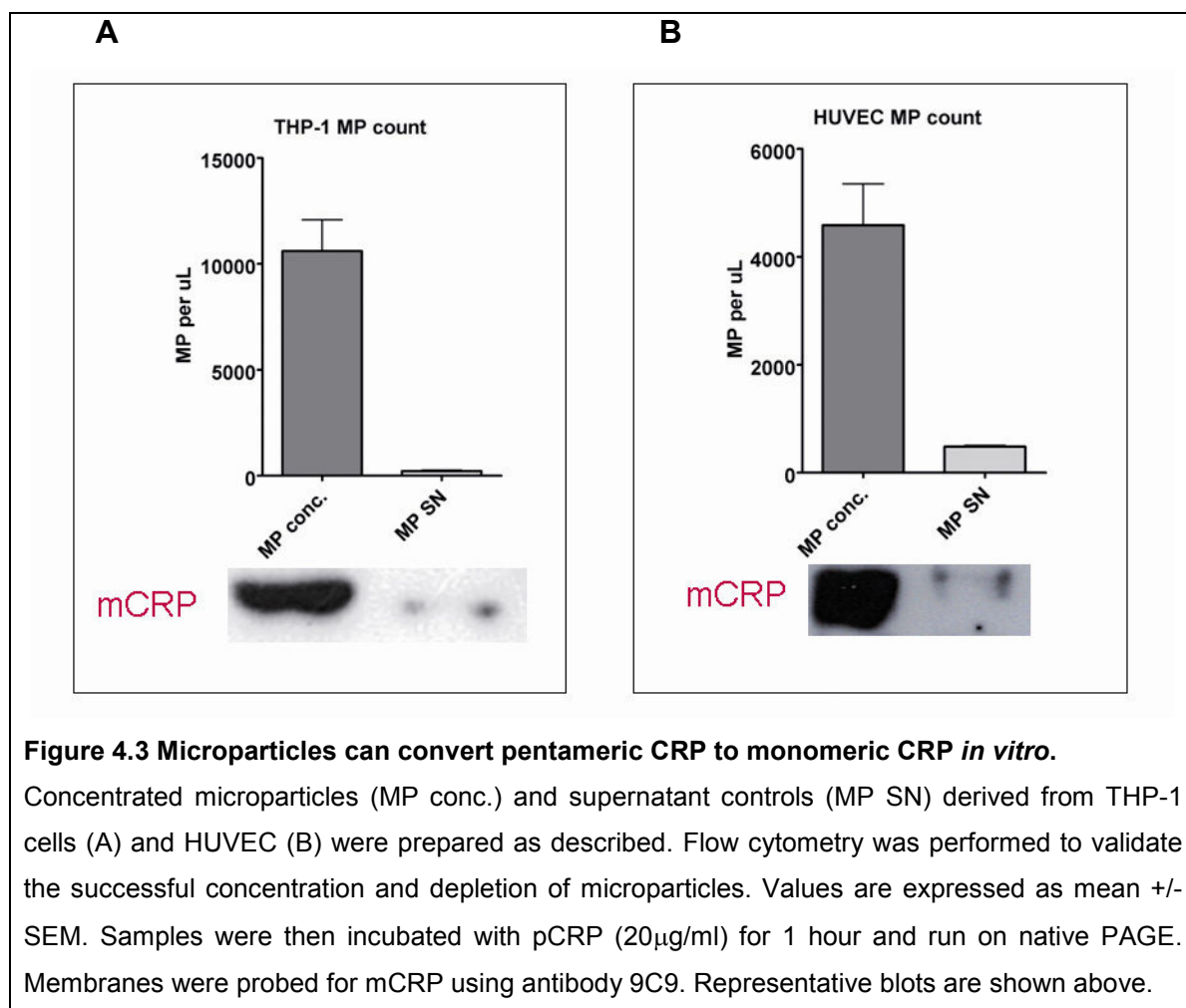


4.1.3 THP-1- and HUVEC-derived microparticles dissociate pentameric CRP to monomeric CRP

It has previously been shown that pCRP is converted to mCRP following binding to activated cell membranes (24). As microparticles are shed from activated or stressed cells (30) we hypothesised that they should also be capable of pCRP degradation.

Microparticles were derived from THP-1 and HUVEC following stimulation with LPS and TNF- α respectively. Concentrated microparticles and microparticle depleted supernatant were obtained and incubated with pCRP. Microparticles from both cell types were able to generate mCRP from pCRP which is shown in figure 4.3. The microparticle depleted sample was unable to produce a significant amount of mCRP, which was consistent with the substantially reduced microparticle count as measured by flow cytometry.

The substantial difference between the surface proteins of THP-1 and HUVEC further supports the concept that pCRP dissociation occurs on cell membranes and occurs independently of surface receptors.



4.1.4 Whole blood-derived microparticles dissociate pentameric CRP to monomeric CRP which can be inhibited by 1,6 bis-phosphocholine

The anti-pCRP compound bisPC binds pCRP at its phosphocholine (PC) binding site. It acts to bind two CRP pentamers together to form a decamer in a molar ratio

of 5 bisPC : 2 pCRP (78). Given the central importance of PC binding in the dissociation process of pCRP to mCRP, it was investigated whether this compound could inhibit the formation of mCRP.

Concentrated microparticles were prepared from whole blood following incubation with ADP. They were then incubated for an hour with pCRP or pCRP combined with varying molar ratios of bisPC (figure 4.4 upper panel) or compared to microparticle depleted plasma (figure 4.4 lower panel).

The addition of pCRP to mixed whole blood microparticles results in the formation of mCRP. This process did not occur in the microparticle depleted supernatant control. Furthermore, pre-incubation of pCRP with bisPC was able to inhibit the formation of mCRP in a concentration dependent manner. BisPC prevents pCRP ligand binding by engaging the PC binding site; therefore this result provides further support to the concept that ligand engagement is required for pCRP dissociation.

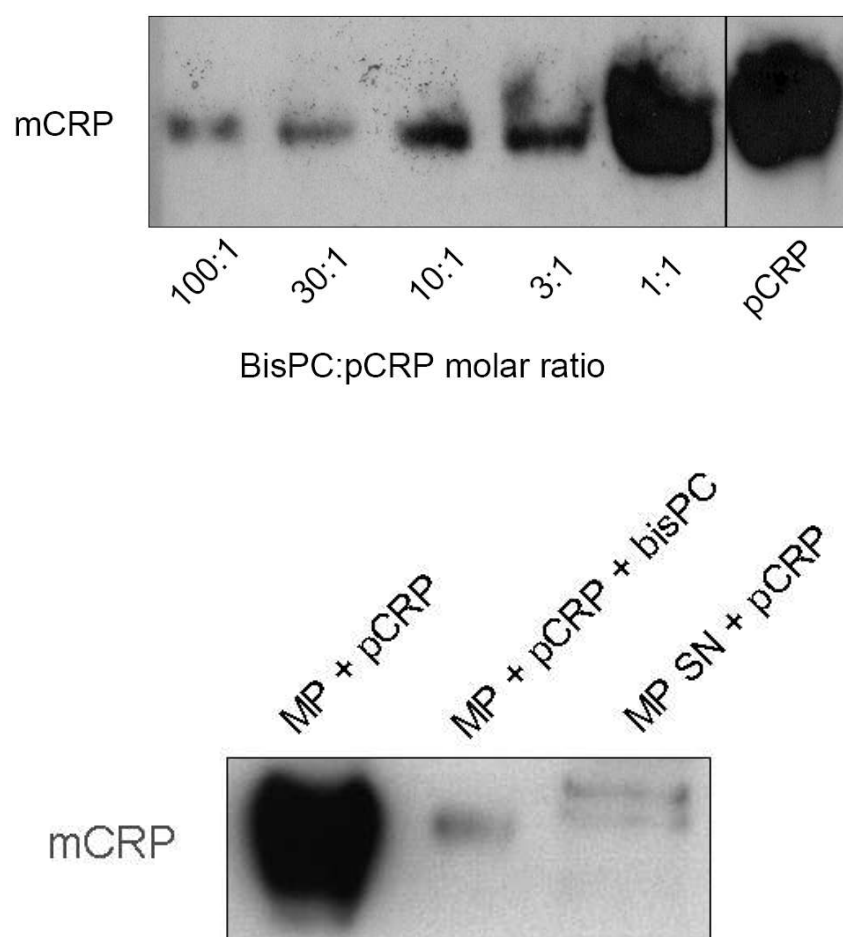


Figure 4.4 Human blood-derived microparticles can convert pentameric CRP to monomeric CRP *in vitro*.

Upper panel: Western blot demonstrating bisPC inhibiting the conversion of pCRP to mCRP. With a large molar excess of bisPC mCRP formation is significantly inhibited in a concentration dependent manner. **Lower panel:** Microparticles isolated from whole blood convert pCRP to mCRP (MP + pCRP). This process can be inhibited by incubation of pCRP with bisPC (30:1 molar ratio). Microparticle supernatant (MP SN) depleted of microparticles is unable to produce significant amounts of mCRP.

4.2 Monomeric CRP in the context of myocardial infarction

4.2.1 Monomeric CRP can be detected on circulating microparticles following myocardial infarction

mCRP has previously been detected in atherosclerotic plaques (24) and in peri-infarct regions of brain tissue following cerebrovascular accidents (79). However, there have not been any reports of mCRP detected in the circulation or through methods other than histology. Following acute myocardial infarction circulating pCRP levels rise consistently in association with the size of myocardial infarction

(12). Following the *in vitro* demonstration that microparticles can convert pCRP to mCRP, it was investigated whether mCRP could be detected on circulating microparticles in patients following primary PCI for myocardial infarction.

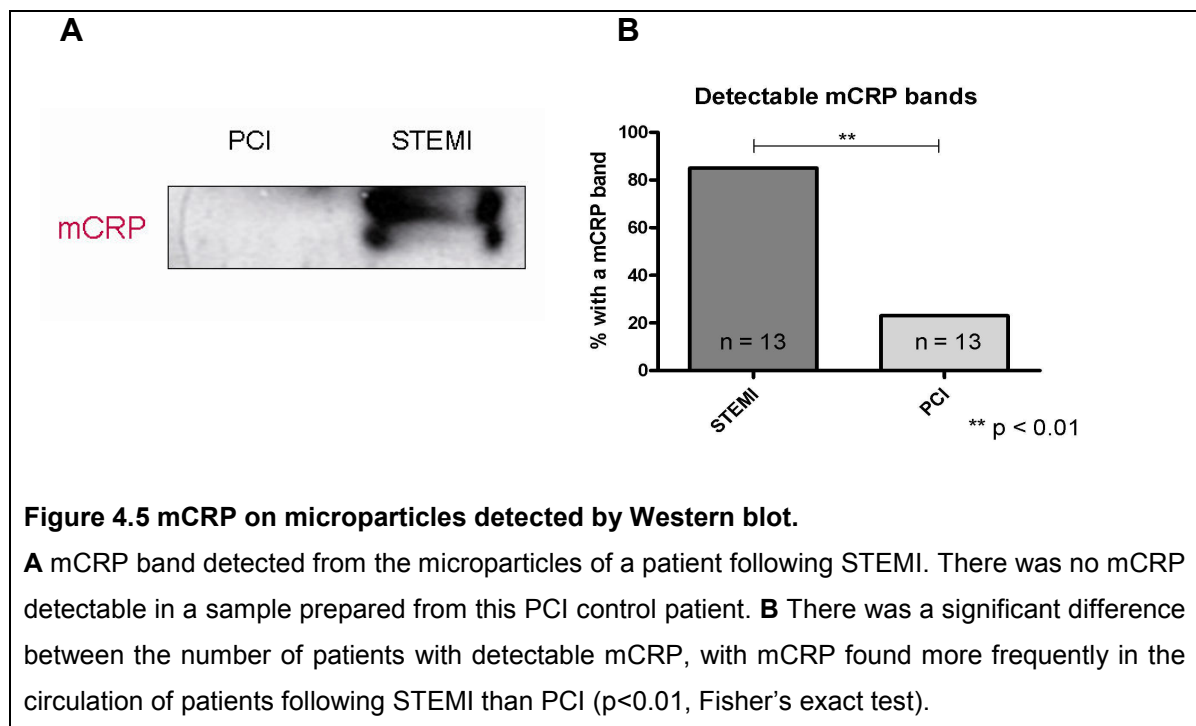
For this study patients with a documented STEMI were recruited. All patients in the STEMI group underwent primary PCI with successful restoration of flow following occlusion of a major coronary vessel. A second group of patients who also underwent PCI with stent deployment but did not present to hospital with a STEMI were also included as procedural and treatment controls.

Patient characteristics were comparable across the two groups as shown in table 4.1. Patients with a STEMI had higher troponin, creatinine kinase (CK) and (p)CRP. They were also slightly younger but otherwise there were no significant differences between the two groups; of note there was no significant difference in the use of anti-platelet agents or statin therapy. Collected samples were analysed by Western blotting and FACS for the presence or absence of mCRP.

	STEMI (n=13)	PCI Control (n=13)	
Demographics			
Age	58.1 +/- 9.5	66.7 +/- 7.7	p<0.02*
Sex (M)	85%	77%	p=1#
Clinical values			
CRP	35.8 +/- 33.6	10.0 +/- 15.5	p<0.001\$
Troponin	97.2 +/- 121.5	0.8 +/- 0.7	p<0.001\$
Creatinine Kinase	2901 +/- 2109	176 +/- 57	p<0.001\$
Creatinine	80.8 +/- 22.5	82 +/- 18.0	p=0.12\$
Drug eluting stent	23%	62%	p=0.11#
Risk Factors			
Smoker	54%	23%	p=0.22#
Hypertension	54%	69%	p=0.69#
Diabetes Mellitus	23%	31%	p=1#
Family History	38%	23%	p=0.67#
Elevated Cholesterol	46%	85%	p=0.10#
Medication			
Aspirin	100%	100%	p=1#
Clopidogrel	100%	100%	p=1#
Statin	100%	100%	p=1#
IIb/IIIa inhibitor	15%	31%	p=0.65#

Table 4.1 Clinical and demographic characteristics of STEMI and PCI control groups.
 Symbols following p values denote statistical test used: * t-test, # Fisher's exact test, \$ Mann-Whitney rank sum.

mCRP was detected on the majority of microparticle isolates from patients with a STEMI (10/13, 77%). A representative blot is shown in figure 4.5A. mCRP was also detected in a small number of patients who had undergone PCI (3/13, 23%) with a significant difference between the two groups (p<0.05, Fisher's exact test, figure 4.5B).



Microparticle analysis performed by flow cytometry provided complimentary data. Following a STEMI the mean mCRP fluorescence was 525 ± 72 (SEM). This was significantly higher than the value of 282 ± 65 (SEM) in control patients who had undergone PCI without having a STEMI ($p < 0.02$). This data is shown in figure 4.6 with a representative flow cytometry histogram. These results were not significantly affected if normalised for circulating microparticle numbers.

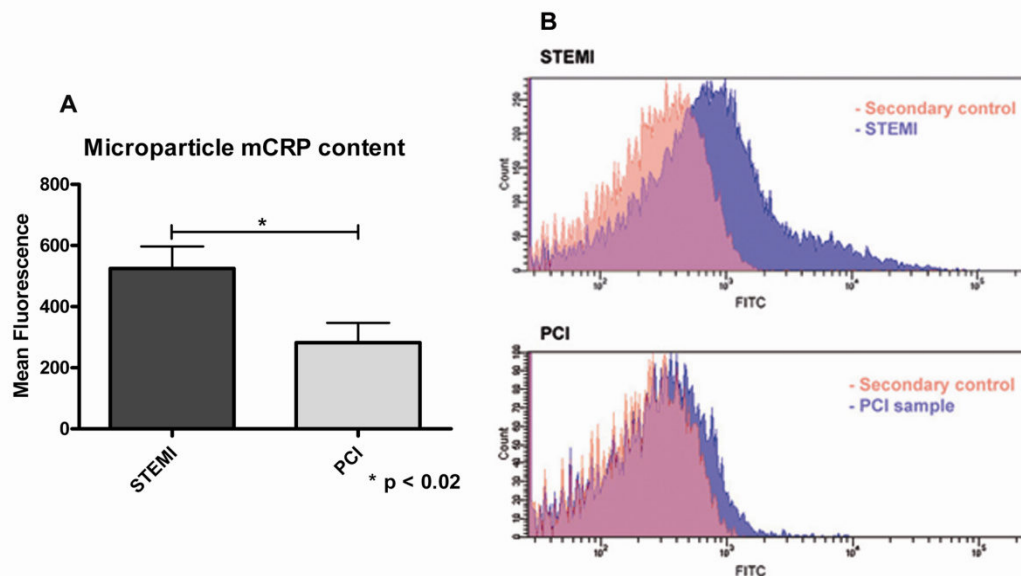


Figure 4.6 mCRP on microparticles analysed by flow cytometry.

A Microparticles were analysed by flow cytometry. There was significantly more mCRP detected on microparticles in patients following a STEMI compared to those who had only undergone PCI ($p < 0.02$, 2 tailed t-test). **B** Representative flow cytometry histograms from each patient group with secondary control shown.

4.3 Monomeric CRP in the context of Alzheimer's disease

4.3.1 Characterization of artificial beta-amyloid plaques

The artificial plaques formed via aggregation of $A\beta_{42}$ peptide form beta sheet structures similar to $A\beta$ plaques and can therefore serve as a model for the plaques found in the brain of Alzheimer's disease patients. Thioflavin T has the property of emitting a green fluorescence after excitation at 485 nm, when bound to beta sheet structures, and thus indicates the presence of beta sheet structures. Artificial plaques but not the non-aggregated $A\beta_{42}$ peptide demonstrated this characteristic (Figure 4.7).

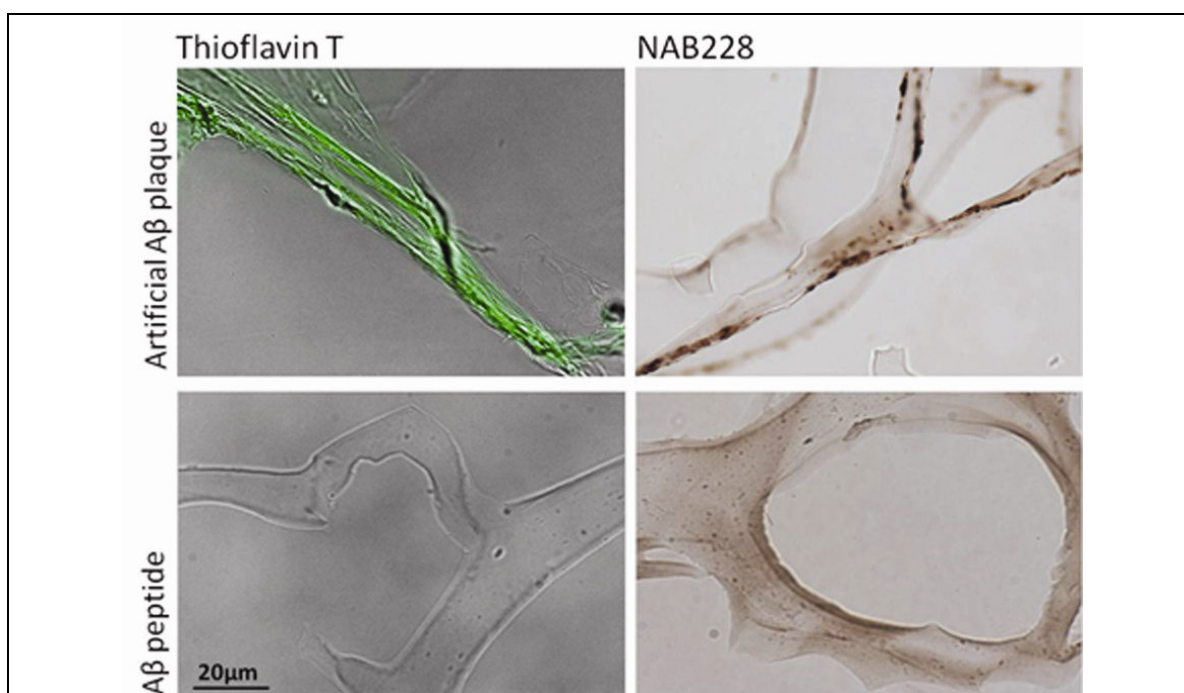
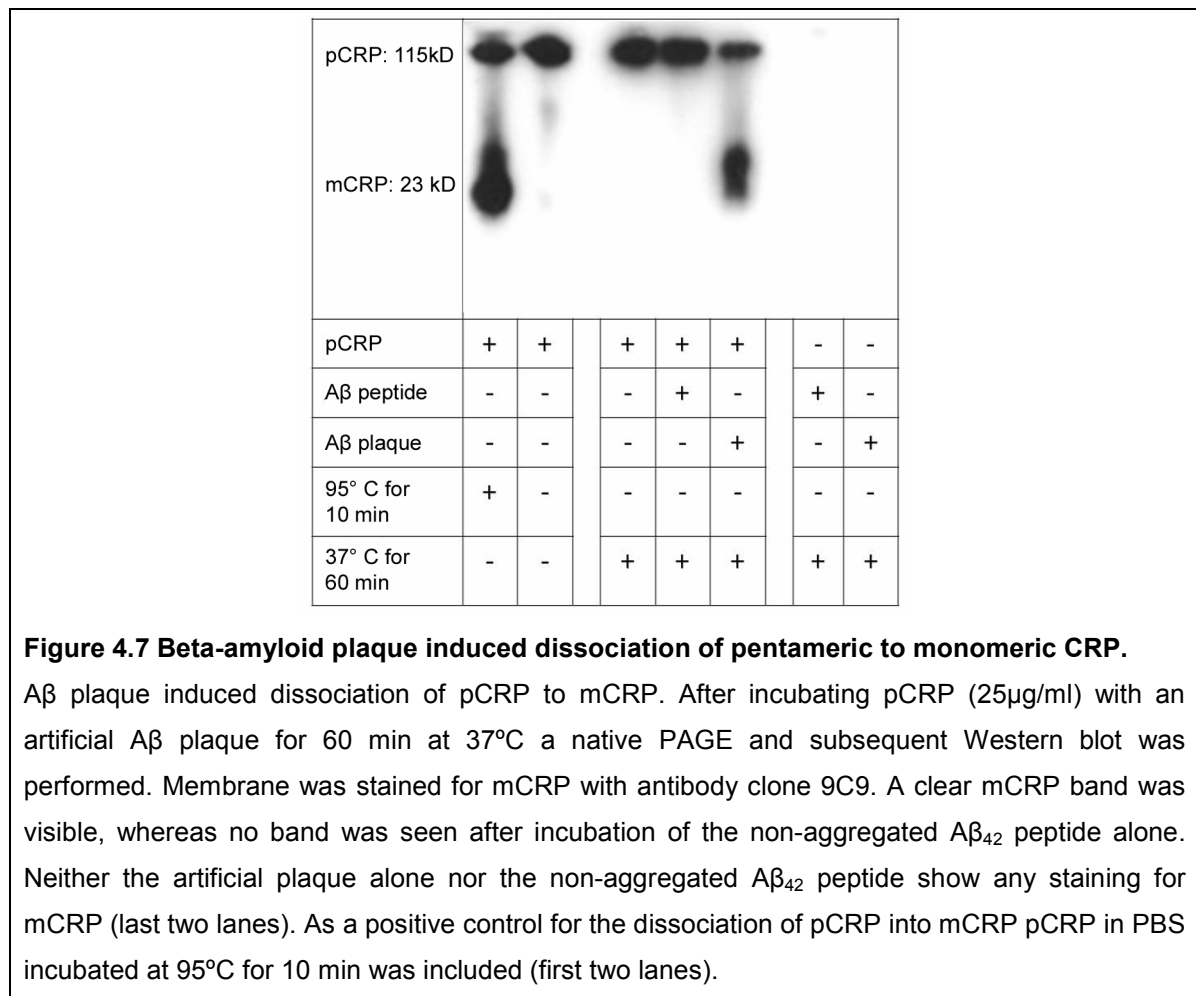


Figure 4.7 Characteristics of artificial beta-amyloid plaques.

Artificial plaques formed through aggregation of A β ₄₂ peptide form beta sheet structures and can therefore serve as a model for the plaques found in the brain of patients with Alzheimer's disease. The presence of beta sheet structures is shown by thioflavin T binding and subsequent emission of green fluorescence. **Left column:** Artificial plaques and non-aggregated A β peptide in agarose were stained with 3 mM thioflavin T solution and pictures were taken at excitation and emission wavelengths of 485 and 550 nm, respectively. Green fluorescence can be seen in artificial plaques, but not in A β ₄₂ peptide. **Right column:** Artificial plaque or A β ₄₂ peptide in agarose stained with monoclonal antibody NAB228 against beta-amyloid. Staining for beta-amyloid can be seen in both peptide and artificial plaque. In the sections of the non-aggregated peptide staining is evenly distributed in the agarose, whereas aggregates can be seen in the sections with the artificial plaque.

4.3.2 Beta-amyloid plaques dissociate pentameric CRP to monomeric CRP

A β plaque formed *in vitro* and un-aggregated peptide that had not undergone plaque formation were incubated with pCRP for 1 hour at 37° C. The contents were then analyzed for the presence of mCRP using native Western blot. This blot demonstrated mCRP formation induced by A β plaques, however the peptide alone was not able to dissociate the pentameric isoform of CRP to its monomeric isoform (figure 4.7).



In a separate experiment A β plaque was also incubated with pCRP, fixed in agarose and sectioned for immunohistological staining. Clone 9C9 (mCRP specific) and clone 8D8 (pCRP specific) were used to identify CRP isoforms. Strongly positive staining (brown colour) is visible for slides treated with 9C9, whereas almost no staining is detectable in those with 8D8 staining (figure 4.8). Control experiments performed to exclude the possibility of non-specific binding to A β plaque confirmed the specificity of the primary and secondary antibodies used. Finally, plaques were stained with the antibody clone NAB228 to confirm the homology between the plaques generated *in vitro* and those found *in vivo* (figure 4.8).

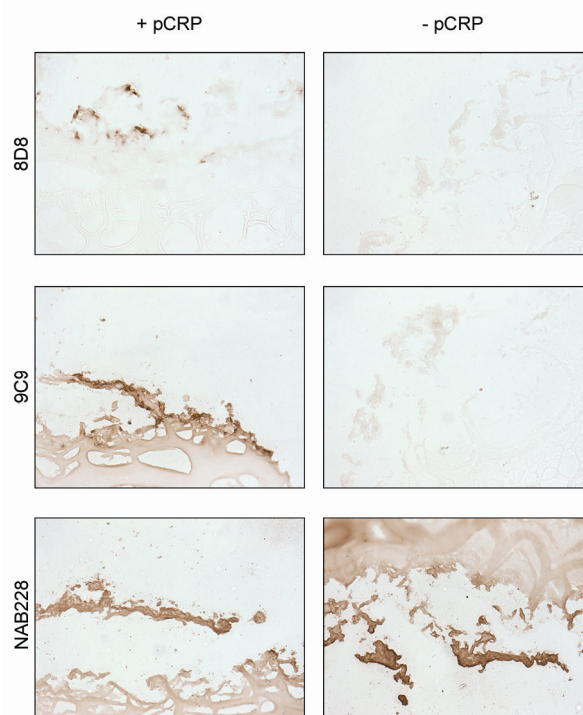


Figure 4.8 Histological proof of monomeric CRP generation by an artificial beta-amyloid plaque.

An artificial A β plaque incubated with pCRP (left lane) and fixed in agarose showing positive (brown) staining with antibody clones 8D8 (pCRP), 9C9 (mCRP) and NAB228 (beta-amyloid). Another artificial plaque incubated without pCRP (right lane), fixed and stained showed no staining for 8D8 or 9C9. Positive staining (brown) is seen with NAB228.

4.3.3 Beta-amyloid plaques induce platelet activation

To demonstrate the pro-inflammatory effects of A β plaques as published previously (80-81) PRP were pre-incubated with either the artificial plaque (10 μ M final concentration), PBS or pCRP (10 μ g/ml final concentration) for 15 min at 37°C. Afterwards the ability of each sample to activate platelets was measured by aggregometry as described under methods. A representative result is shown in figure 4.9a.

The experiment not only confirmed the results by Herczenik *et al.* that mis-folded proteins have the capacity to activate platelets (figure 4.9b) but also observed the ability of pCRP to prevent platelet activation.

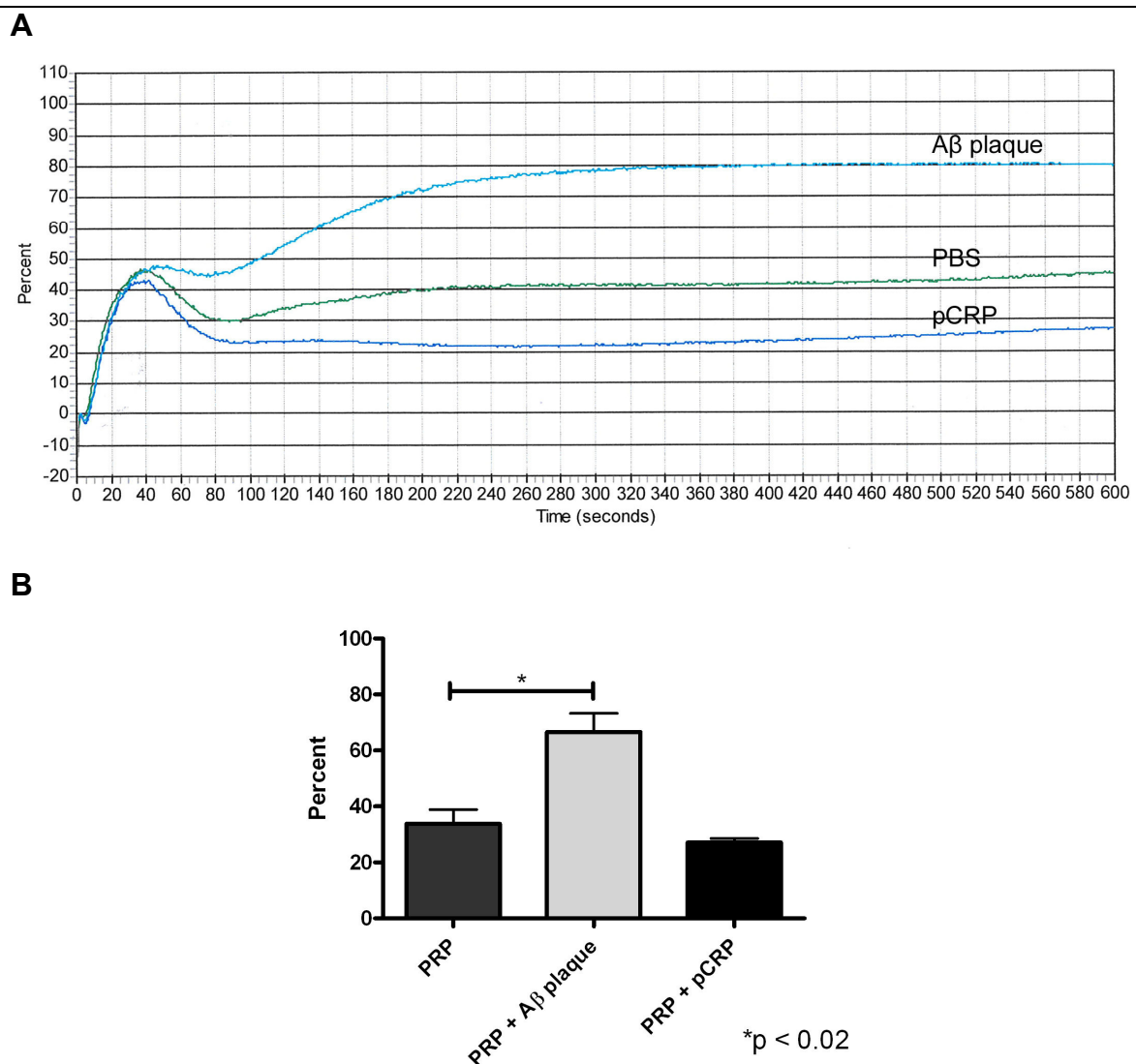


Figure 4.9 Beta-amyloid plaques activate platelets as shown by aggregometry.

A Light transmission aggregometry demonstrates platelet activation in percent over a time period of 10 minutes. The light blue line is platelet rich plasma (PRP) pre-incubated with beta-amyloid plaque and shows an 80 percent increase in light transmission. The green line is PBS only where there is an increase of 45 percent. Interestingly, in the PRP sample pre-incubated with pCRP there appears to be an inhibitory effect where there is a 30% increase in light transmission.

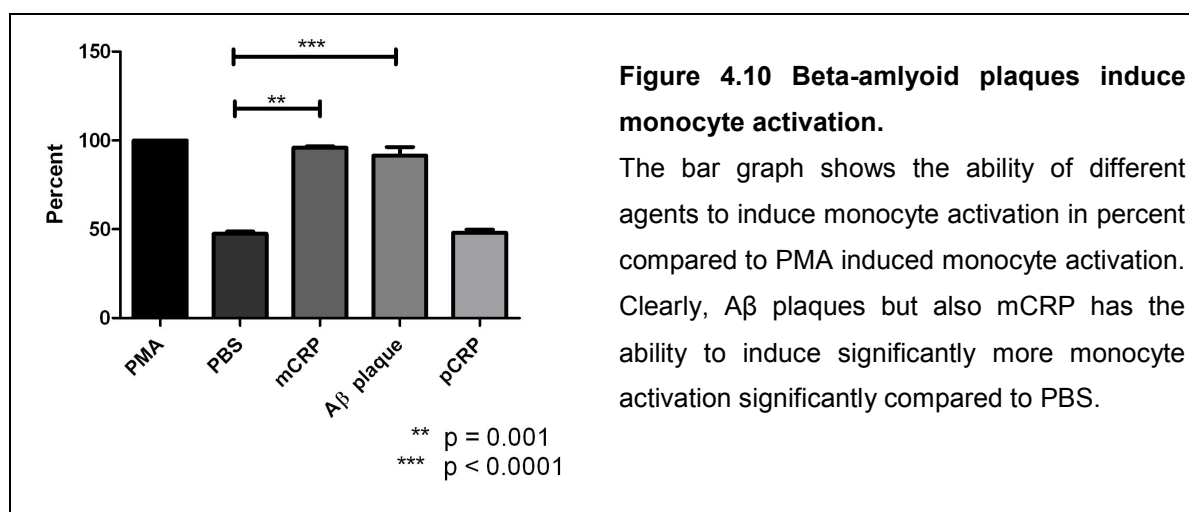
B Platelet activation analysed by aggregometry show that significant more platelets get activated when pre-incubated with Aβ plaque compared to PRP only or PRP pre-incubated with pCRP ($p < 0.02$). Note the inhibitory effect of pCRP.

4.3.4 Beta-amyloid plaques induce monocyte activation

Other authors have previously shown the pro-inflammatory effects of Aβ plaques by demonstrating their capacity to induce monocyte migration (82). A similar monocyte adhesion assay was performed as described in the methods section to evaluate if artificial plaques show the same characteristics.

Isolated monocytes were incubated with either PMA as a positive control, PBS, mCRP (12,5 µg/ml final concentration), pCRP (12,5 µg/ml final concentration) or the artificial plaque (25 µM final concentration) for 30 min at 37°C. PMA as a positive control was assigned to 100 percent activation.

Our artificial plaque showed the same pro-inflammatory characteristics as expected. The artificial plaque was able to induce significantly more monocyte activation compared to PBS ($p = 0.001$). Furthermore, as published before, mCRP induced significantly more monocyte activation when compared to PBS (figure 4.10)



4.3.5 Monomeric CRP but not pentameric CRP can be detected in brain tissue of patients with Alzheimer's disease

Sections of frontal cortex from patients diagnosed with Alzheimer's disease and non-Alzheimer's disease cases were stained with antibody clones 9C9 (mCRP), 8D8 (pCRP) and NAB228 (figure 4.9). Sections from Alzheimer's disease patients were strongly positive (brown colour) for mCRP staining but not for pCRP, whereas neither mCRP nor pCRP could be found in the healthy controls.

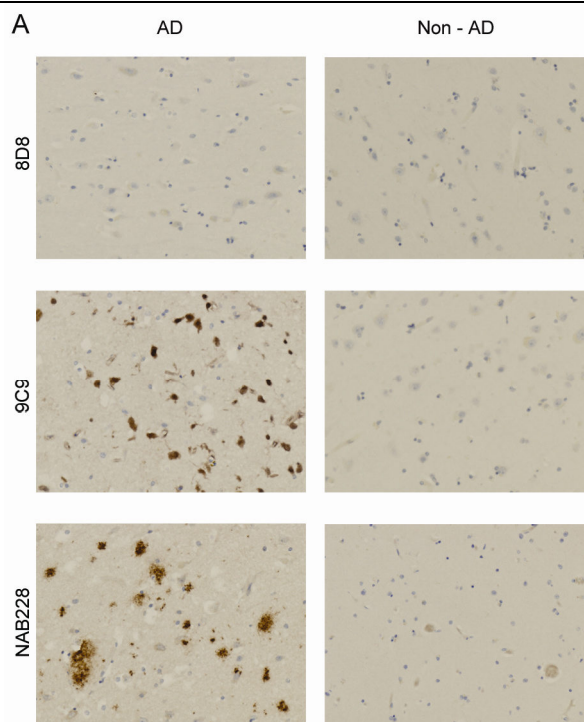


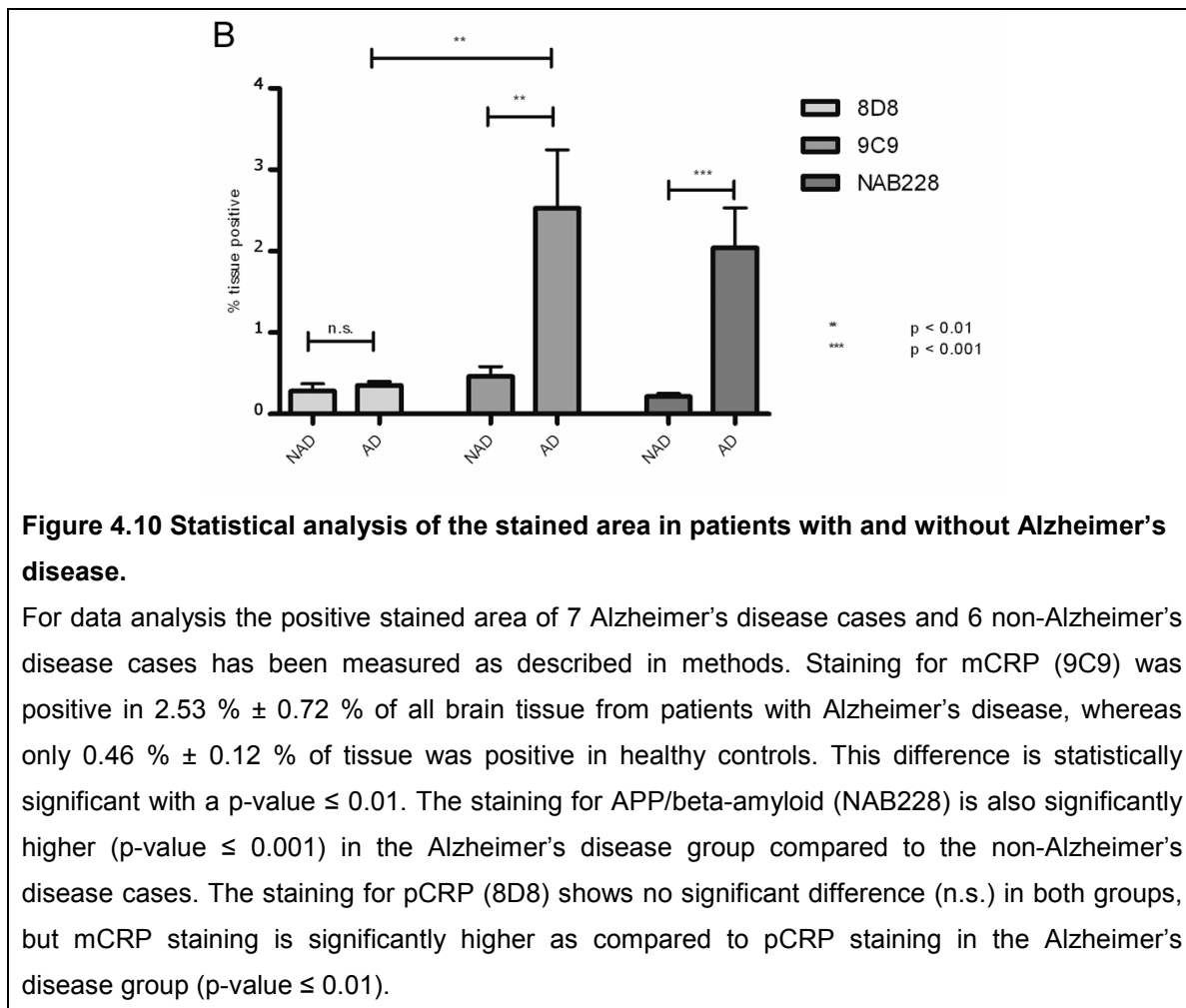
Figure 4.9 Identification of mCRP but not pCRP in human brain tissue from Alzheimer's disease patients with beta-amyloid plaques.

Human brain tissue from the frontal cortex from a patient with Alzheimer's disease (left lane) demonstrates positive staining (brown) with the antibody clones 9C9 (mCRP-specific) and NAB228 (beta-amyloid-specific), whereas almost no staining is detectable with clone 8D8 (pCRP-specific). In contrast, almost no staining is visible in the human brain tissue from a healthy control (right lane) for the antibody clones 8D8, 9C9 or NAB228. These images are representative of observations for 7 Alzheimer's disease cases.

Clone NAB228 was used to identify the distribution pattern of the A β plaques and confirm their presence in the samples obtained from Alzheimer's disease patients. All patients assigned to the Alzheimer's disease group had significant plaque burden on histological staining.

The area with positive staining in all sections was quantified using Image-Pro® Plus (figure 4.10). $2.53\% \pm 0.72\%$ of the cortex of Alzheimer's disease patients were positive for mCRP, whereas only $0.46\% \pm 0.12\%$ of the cortex of the controls were positive ($p < 0.01$). There was only a small amount of pCRP detected in sections from Alzheimer's disease patients as well as in controls ($0.35\% \pm 0.05\%$ vs. $0.28\% \pm 0.09\%$ respectively, p not significant). Comparison of total mCRP and pCRP staining demonstrated significantly more mCRP than pCRP ($2.53\% \pm 0.72\%$ compared with $0.35\% \pm 0.05\%$, $P < 0.01$). As expected, and similar to results observed for mCRP formation, A β plaques were far more prevalent in sections

from Alzheimer's disease patients when compared to controls ($2.04\% \pm 0.49\%$ vs. $0.22\% \pm 0.04\%$ respectively $p \leq 0.001$).



4.3.6 Monomeric CRP co-localizes with complement component C1q in the cortex of patients with Alzheimer's disease

Sections of the frontal cortex from patients diagnosed with Alzheimer's disease and from non-Alzheimer's disease cases were stained with the antibody clone 9C9 (mCRP) and antibody H-55 (C1q). Samples were then stained with anti-mouse or anti-rabbit fluorochrome labelled secondary antibodies (Figure 4.11). Sections from Alzheimer's disease patients showed positive staining for mCRP (red fluorescence) and for C1q (green fluorescence) and co-localization can be seen in the overlays, whereas neither mCRP nor C1q could be found in the healthy controls.

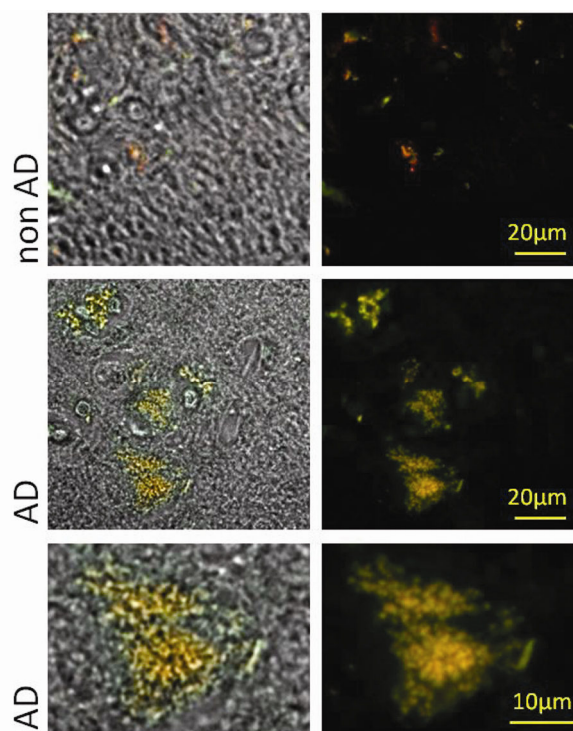


Figure 4.11 Monomeric CRP and C1q co-localization.

mCRP (red staining) and C1q (green staining) are co-localized in human brain tissue of patients with Alzheimer disease. In contrast, there is almost no staining for mCRP or C1q in brain tissue of healthy controls. mCRP was detected with antibody clone 9C9 and Alexa fluor 555 labelled secondary antibody. C1q was detected with rabbit mAb against C1q and Alexa fluor 488 labelled secondary antibody. The left column shows overlays of bright field and fluorescence pictures taken at 60x magnification. The right column shows fluorescence pictures only. The bottom row shows the co-localization of mCRP and C1q at higher magnification (note the different scale bars).

4.3.7 Monomeric CRP co-localizes with beta-amyloid plaques in the cortex of patients with Alzheimer's disease

mCRP detected by staining with antibody clone 9C9 and Alexa fluor 555 labelled anti-mouse secondary antibody is co-localized with A β plaques in sections of the frontal cortex from patients with Alzheimer's disease (Figure 4.12). A β plaques have been detected by thioflavin T binding and subsequent imaging at excitation and emission wavelengths of 480 and 550 nm, respectively. There was no staining for mCRP and no fluorescence detectable following thioflavin T staining in non-Alzheimer's disease controls.

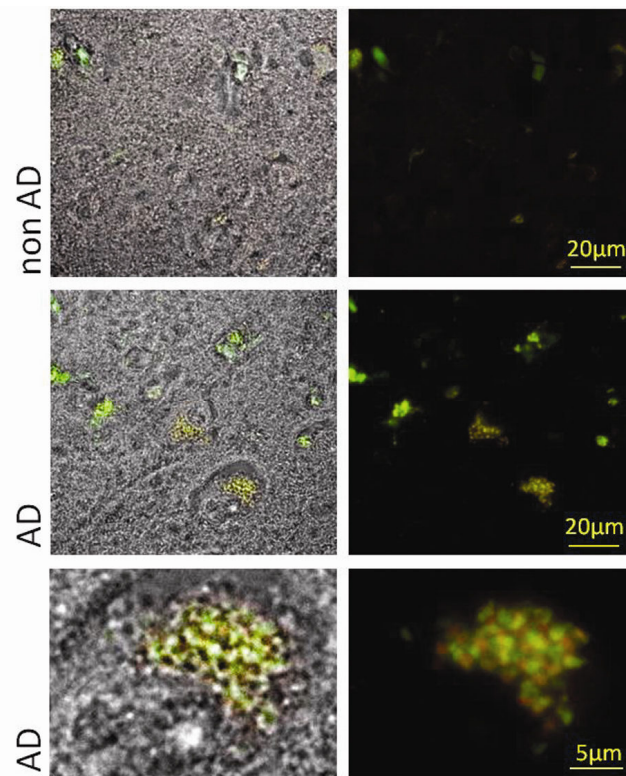


Figure 4.12 Monomeric CRP and beta-amyloid plaques co-localization.

mCRP (red staining) co-localizes with β -amyloid plaques (green staining) in the brain of patients with Alzheimer's disease. Plaques were identified by staining with thioflavin T and fluorescence imaging at an excitation and emission wavelength of 485 and 550 nm, respectively. mCRP was detected with antibody clone 9C9 and Alexa fluor 555 labelled secondary antibody. No β -amyloid plaques and almost no staining for mCRP are visible in tissue of healthy controls. The left column shows overlays of bright field and fluorescence pictures taken at 60x magnification. The right column shows fluorescence pictures only. The bottom row shows the co-localization of mCRP and A β plaques at higher magnification (note the different scale bars).

5 Discussion

5.1 Monomeric CRP in the context of myocardial infarction

This thesis demonstrates that the dissociation process of pentameric C-reactive protein (pCRP) to monomeric subunits (mCRP) occurs following its binding to microparticles. This finding is consistent with the previous discovery that this process takes place on activated cell membranes, either model systems (24-25) or *in vitro* (24). Furthermore, the thesis demonstrates for the first time that mCRP can be detected on circulating microparticles isolated from peripheral blood samples in patients following myocardial infarction. This finding is consistent with a recent study that also identified CRP on circulating microparticles (84), however in this study the conformational status was not assessed. This is the first study in which mCRP specifically has been detected in the circulation of a patient population. This is a critical advance in establishing the biological relevance of this isoform and may resolve some of the conflicts currently surrounding the pathological role of CRP.

Although circulating (p)CRP levels have been shown to correlate with the individuals' cardiovascular risk (9), population studies investigating a direct causal role have generally been inconclusive (23). This is despite the fact that CRP has been detected in atherosclerotic plaques (85), infarcted myocardium (86) and has been shown to have broad pro-inflammatory effects on vascular endothelium (87). Following myocardial infarction the peak plasma level of CRP has been shown to correlate with infarct size (12, 88), development of heart failure (6) and mortality (6-8). A pioneering study measuring local biomarker concentrations found that CRP levels in occluded coronary arteries are significantly reduced compared to the systemic circulation. This finding suggests local deposition and catabolism (11); supporting the hypothesis that CRP plays an active pathological role following myocardial infarction. In a rat model of myocardial infarction infusion of pCRP at physiologically relevant concentrations has been shown to increase infarct size in a complement dependent manner by 30-50% (10, 78). This result was confirmed following the development of the novel anti-CRP agent bisPC which acts to bind two pCRP molecules together to form a stable decamer. Infusion of this agent was also able to completely reverse myocardial cell death exacerbated by CRP in a similar rat myocardial infarction model (78). However,

the mechanism required for CRP activation and subsequent complement fixation in this setting remains elusive.

The dissociation of pCRP to mCRP is a plausible potential mechanism to resolve this dichotomy. Although the ability of pCRP to dissociate to individual monomers with unique biological properties was recognised previously (89) the relevance of this process to biological systems has not been fully explored (19, 90). The notion that mCRP is generated *in vivo* is supported by previous identification of auto-antibodies directed against mCRP in patients with systemic lupus erythematosus (91) and tubulointerstitial nephritis and uveitis syndrome (92). mCRP itself has been identified in regions of stroke (79), atherosclerotic plaques (24) and brain tissue of patients with Alzheimer's disease (93).

The mechanism by which pCRP is dissociated into monomers following binding to microparticles remains elusive and has not been determined in this thesis. But previous work showing the dissociation on activated cell membranes and model systems suggests a non-receptor mediated signalling pathway. The surface of cell membranes alters upon activation (94) and *in vitro* studies showed that these newly formed surfaces seems to be capable of initiating dissociation. Mostly lysophosphatidylcholine which plays a key role in triggering the dissociation of pCRP to mCRP as unpublished data shows the inhibition of mCRP formation by activated platelets using a phospholipase A₂ inhibitor. As microparticles inherit the cell membrane surface from their cell of origin it is most likely that the same membrane proteins are responsible for inducing the dissociation.

The demonstration of a plausible mechanism of *in vivo* formation of mCRP (24) coupled with the discovery that mCRP can be detected on microparticles potentially marks a paradigm shift in our understanding of the pathogenic effects of CRP in inflammation (95). This is because mCRP has significant pro-inflammatory properties not shared with pCRP. These include complement component C1q fixation (25, 96), monocyte activation (24) and thrombus formation (26). The interaction between mCRP and complement is most significant as it has been shown that CRP induced tissue damage is entirely dependent on complement activation (10, 78). However, pCRP has not been shown to have any significant interaction with either complement (96) or complement regulatory factors such as Factor H (19); either surface bound or in the fluid phase. Conversely, these studies show significant interactions between components of the complement system and mCRP. The identification of mCRP in patients with myocardial infarction and

recognition of its pro-inflammatory properties establishes the mechanistic basis underlying the direct pathogenic effects of CRP which have been previously documented (10, 78). Local formation of mCRP on activated membrane surfaces resolves two central issues. A structural change of pCRP to mCRP following membrane binding leads to a functional change including complement fixation. This process also acts to limit CRP driven inflammation to specific regions of damaged tissue, preventing generalised thrombosis.

It remains to be determined what functional role mCRP on circulating microparticles may have. Microparticles have been implicated in numerous pathological processes central to the progression of atherosclerosis (35). It has been demonstrated that microparticles can transfer antigens to the surface of endothelial cells and that these antigens can modify immune responses (97). Platelet-derived microparticles are also capable of triggering inflammatory responses via interleukin-1 signalling (98). These results clearly show that microparticles are capable of mediating intercellular interactions and indeed are required for some inflammatory processes (98). It is certainly possible that microparticles may play a similar role disseminating mCRP in a paracrine fashion, although this has not been determined in this thesis and awaits further investigation.

The demonstration that 1,6 bis-phosphocholine (bisPC) inhibits the formation of mCRP is also a significant discovery. It confirms that pCRP dissociation is dependent on membrane binding, a process that is specifically inhibited by bisPC (78). It also supports the intriguing possibility that bisPC inhibits the activity of pCRP through prevention of mCRP formation; rather than direct inhibition of pCRP. Although this is a novel concept (99), it is supported by studies demonstrating the interaction between mCRP and complement (25). Importantly, this finding also demonstrates a potential therapeutic approach that may be used to limit ischaemic tissue damage following myocardial infarction. CRP is an attractive therapeutic target as serum levels rise only in the hours following infarction, by which time the majority of patients have presented and undergone reperfusion therapy. Furthermore, CRP deficiency has not been associated with any clinical disorder minimising the potential complications of any specific CRP targeted therapy.

The identification of mCRP on circulating microparticles isolated from peripheral blood samples is a significant discovery. It is the first time mCRP has been

isolated from blood and validates much of the previous work that had postulated a plausible mechanism by which this process occurs. By invoking an intermediary conformational change that alters CRP function, it is possible to reconcile previously conflicting observations regarding the role of CRP in inflammation and myocardial infarction. This not only improves our understanding of the pathological processes involved in myocardial infarction but also identifies mCRP as a potential therapeutic target. The approaches of pCRP or mCRP inhibitors are wide spread. The target can either be the mCRP itself or its precursor pCRP as outlined by bisPC in this work. A recent discovered RNA aptamer specifically targeting mCRP (100) showed another method to inhibit the pro-inflammatory mCRP. An alternate therapeutical approach can be monoclonal antibodies specific against mCRP or pCRP as they are widely used in different kinds of diseases. The development of specific pCRP or mCRP inhibitors would not only assist in the determination of specific effects but also appear a promising therapeutic strategy in both myocardial infarction and atherosclerosis.

5.2 Monomeric CRP in the context of Alzheimer's disease

This thesis demonstrates that the monomeric isoform of CRP and not the pentamer is associated with beta-amyloid (A β) plaques found in the cortical tissues from patients with Alzheimer's disease. Furthermore, the thesis was able to provide a mechanistic basis for this discovery; A β plaques but not A β peptides are able to dissociate pCRP into individual monomers. Previous studies have shown the presence of CRP in the brain tissue of Alzheimer's disease patients using non-specific antibodies to detect CRP (17, 101-102). This study using conformation-specific antibodies demonstrates that it is mCRP, not pCRP, which is associated with A β plaques.

The source of CRP identified in the brain is still uncertain. The majority of circulating CRP is synthesised in the liver (90); controlled by cytokines including interleukin-6, tumour necrosis factor- α and interleukin-1. Other potential sources such as atherosclerotic plaques (103) have been identified but the significance of their contribution remains to be elucidated. In brain tissue the pathophysiology is more complicated due to the requirement of systemically produced CRP to cross the blood-brain barrier (BBB) to reach the cerebrospinal fluid (CSF) and brain tissue. However, it has previously been established that during inflammatory

conditions the BBB becomes dysfunctional, enabling proteins normally only found in serum to enter the CSF (104). Elevated serum CRP levels in Alzheimer's disease have been described in several studies (105-107) and are associated with more rapid progression of the disease (108). Although transit of circulating CRP across the BBB is the most likely potential source of cerebral CRP, there are also studies that suggest that it may be produced *in situ*. In 2000 Yasojima *et al.* found that CRP mRNA is up regulated in cells within the affected areas of Alzheimer's disease brains (101); potentially obviating the need to transit the BBB. Additionally, in 2005 Ciubotaru *et al.* showed mCRP production by U937-derived macrophages (109). It is therefore possible that microglia, which function as the resident macrophages of the brain, produce mCRP locally. However, which of these mechanisms operate *in vivo* and their relative importance remains to be established.

In this study it is shown that A β protein which has aggregated into plaques *in vitro* has the capacity to dissociate pCRP to mCRP. In contrast, individual peptides that have not undergone plaque formation cannot dissociate pCRP. The physiological mechanism resulting in pCRP dissociation on A β plaques is not known yet. One potential cause is the displacement of calcium (Ca) bound to pCRP by A β plaques. Ca²⁺ chelation is a well recognised CRP dissociative mechanism (110). Ca²⁺ has been shown to co-accumulate with A β plaques (111) and the donation of the pCRP bound Ca to the plaque may lead to pCRP dissociation (90). An alternate aetiology would be conversion on the membranes of activated cells associated with the A β plaque. Activated cell membranes are currently considered the primary mediator of pCRP dissociation (99) and it is therefore likely that this mechanism also is involved in mCRP formation in Alzheimer's disease. It is most likely that both mechanisms contribute to the dissociation process. Nevertheless, it is the first time a specific protein rather than activated cell membranes was identified as a catalyst for pCRP dissociation.

The pathophysiological role played by CRP in Alzheimer's disease remains an area of significant research interest. In animal models, the intra-cerebroventricular injection of CRP has been shown to be a potent initiator of intra-cerebral inflammation leading to progressive long term memory loss (112). Previous work has established the importance of complement in mediating the pro-inflammatory effects of CRP (10). In 1992 Rogers *et al.* showed co-localization of C1q, membrane attack complex (MAC) and thioflavin S-positive senile plaques (70) *in*

vivo in immunohistochemistry. This is consistent with findings of this thesis as this thesis shows that mCRP is co-localized with thioflavin T-positive senile plaques (figure 4.12) and co-localized with complement C1q (figure 4.11). The pathological role of the complement system in Alzheimer's disease is still unresolved (113). Interestingly, in 2006 Ji *et al.* showed C1q fixation by surface bound mCRP, which regulates the classical complement pathway (CCP) by activating the complement system (114). A study by Biro *et al.* showed that mCRP but not pCRP binds C1q and can activate the CCP (96). It is this distinct functional change initiated upon CRP dissociation that is the crucial intermediate step linking CRP to complement activation. The dissociative process also acts to localize complement activation to areas of plaque formation, accounting for the focal changes observed in pathological studies in Alzheimer's disease.

Additional evidence supporting the central importance of inflammation in degenerative brain diseases has been obtained from a study of traumatic brain injury. In these individuals the initial external impact itself can cause less damage to the brain tissue than the secondary inflammatory response this insult triggers (115). This discovery suggests that anti-inflammatory strategies may be of benefit in the prevention and treatment of degenerative brain diseases, a novel approach with significant potential. Akiyama *et al.* presented a diagram which depicts the role of microglia in the pathogenesis of Alzheimer's disease, inflammation and neuronal degeneration; the scheme was adapted by adding the new findings postulating the role of mCRP in Alzheimer's disease (figure 5.1).

It remains a matter of great controversy whether CRP is a direct mediator of inflammatory processes or merely a marker of systemic inflammation. Animal studies investigating myocardial infarct size after coronary ligation (10) or provoked cerebral ischemia (116) have shown a complement-dependent increase in ischaemic lesion size following infusion with CRP. These findings prompted the development of the first described direct CRP inhibitor, bisPC. This agent was used in a rat model of myocardial infarction and was able to completely inhibit CRP mediated necrosis (78). As pCRP appears to have only limited pro-inflammatory properties, it is more likely that this effect is mediated by blocking its dissociation to the more pro-inflammatory monomeric isoform as shown in this thesis. These findings underline the fundamental significance of the finding that mCRP and not pCRP is found in the brain of patients with Alzheimer's disease.

There are now a large number of observational and experimental studies that have clearly implicated CRP in the development and progression of Alzheimer's disease. However, these studies have not identified the mechanism by which CRP mediates these effects. Introducing the intermediate step of pCRP dissociation to mCRP potentially solves this dichotomy and integrates previously contradictory data.

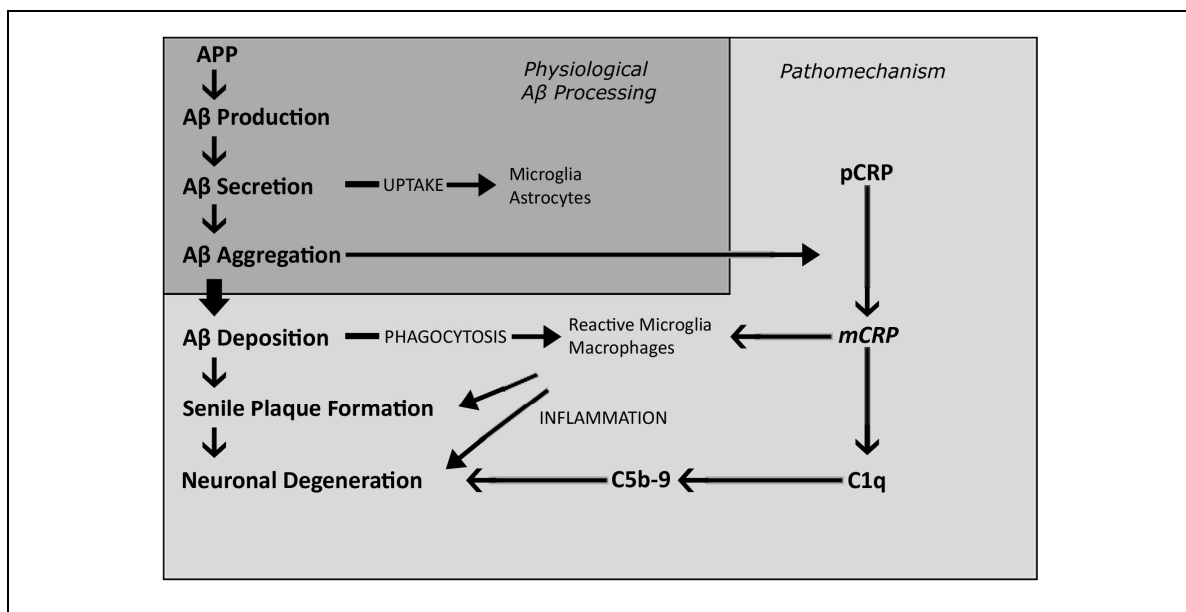


Figure 5.1 The possible role of CRP in the development of Alzheimer's disease.

This adapted scheme describing the pathomechanism of Alzheimer's disease includes a possible role of CRP in the development and neuronal degeneration of Alzheimer's disease. As a first step the Aβ peptide starts to aggregate, which leads to the dissociation of pCRP to mCRP. mCRP itself as a strong pro-inflammatory agent recruits/activates macrophages/microglia and has the ability to fix C1q to start the complement cascade. As a final step C5b-9 known as the membrane attack complex contribute to the neuronal degeneration seen in patients with Alzheimer's disease.

In conclusion, this thesis shows that Aβ plaques can induce the dissociation of pentameric to monomeric CRP and thereby localize inflammation to Aβ plaques. Consistent with this pathophysiological concept, the experiments could identify monomeric CRP together with Aβ plaques in the cortical tissues from patients with Alzheimer's disease. This finding potentially links CRP to the inflammatory processes underlying the progression of Alzheimer's disease and potentially other degenerative brain diseases. This finding contributes to the understanding of the pathophysiology of Alzheimer's disease, and it may enable the development of novel therapeutic approaches for this most insidious disease.

5.3 Limitations of this study

The number of patients and controls in both aspects – mCRP on microparticles following myocardial infarction and mCRP in the pathogenesis of Alzheimer's disease - were relatively small.

Further limitations which need to be addressed are confounding factors as medications and comorbidity in the PCI and STEMI group as well as in patients with Alzheimer's disease and the control group. Even though controlling for potentially confounding factors as gender, age, main risk factors and main medication have been made for the STEMI and PCI control group there is still the possibility for not considered medications with an influence leading to a possible selection bias. The same confounding factors especially the medication could have lead to a possible selection bias regarding the Alzheimer's disease and control group.

We also have to keep in mind that the set up of an artificial beta-amyloid plaque is an *in vitro* experiment and therefore the dissociations process of pCRP to mCRP in patients with Alzheimer's disease might be different *in vivo*. Although we have shown the beta structure (figure 4.7) of the artificial plaque and the approach is well established (72) the circumstances of the *in vivo* plaque are quite different as the plaque is not soluble but fixed in brain tissue and the senile plaque consists of more than the beta-amyloid protein in its beta structure like neurofibrillary tangles, astrocytes and microglia.

6 Summary

C-reactive protein (CRP) is used in clinical practice as a non-specific but sensitive marker for inflammation as serum levels can rise up to 1000-fold from baseline. But it seems that CRP is not only a bystander in inflammation. Elevated CRP levels following myocardial infarction (MI) are associated with poor outcome. Animal studies showed a direct pathogenic role of CRP but the mechanism underlying this remains elusive. An association between circulating CRP and Alzheimer's disease (AD) has also been reported but the pathomechanistic link hasn't been established here either. The missing link in both cases might lay in the dissociation of CRP from its pentameric isoform (pCRP) as found in the circulation into its pro-inflammatory monomeric isoform (mCRP). To test this hypothesis microparticles (MP) were obtained from cell cultures and analyzed for the capacity to dissociate pCRP to mCRP by Western blot. Afterwards patient whole-blood samples following MI and control group whole-blood samples were obtained, MP were isolated and analyzed for mCRP by Western blot and flow cytometry. In order to test the potential of beta-amyloid (A β) plaques, a key player in AD, to induce the dissociation of pCRP to mCRP, pCRP was incubated with A β plaques generated in vitro and with non-aggregated A β ₄₂ peptide. Furthermore, sections of the frontal cortex from brains of patients with and without AD were stained with antibodies specific for mCRP and pCRP. MP showed the ability to convert pCRP to mCRP which could be inhibited by the anti-CRP compound 1,6 bis-phosphocholine. Significantly more mCRP was detected on MP from patients following MI compared to the control group by western blotting and flow cytometry. pCRP dissociation to mCRP was found only when co-incubated with A β plaques, not when co-incubated with the non-aggregated protein. Brain sections from patients with AD showed significantly more mCRP staining compared to healthy controls ($p \leq 0.1$). In contrast, there was no significant difference in pCRP staining. The finding that circulating MP can convert pCRP to pro-inflammatory mCRP in patients following MI is the first time mCRP production has been demonstrated *in vivo*. It is also the first report in which mCRP has been detected in peripheral blood. This supports the hypothesis that mCRP has an active biological role and potentially outlines a novel therapeutic approach in MI.

The capacity of A β plaques to dissociate pCRP to mCRP shows a mechanism which explains the existence of mCRP but not pCRP in the brains of AD patients. This finding reveals the potential of locally generated mCRP to amplify and localize inflammation.

7 Kurzfassung in deutscher Sprache

Einleitung: C-reaktives Protein (CRP) ist ein seit über 80 Jahren bekanntes Protein der Pentraxinfamilie und gehört zu den Akute-Phase-Proteinen. Es wird überwiegend in der Leber, insbesondere nach Stimulation mit Interleukin-6 und den Tumor-Nekrose-Faktor- α , synthetisiert. CRP zirkuliert im menschlichen Blutkreislauf als diskusgeformtes Pentamer (pCRP) bestehend aus 5 gleichen nicht-kovalent gebundenen 23 kDa großen Untereinheiten. Eine Beziehung zwischen verschiedenen Arten der Entzündung und erhöhten CRP-Blutplasmawerten konnte bereits nachgewiesen werden. Erst vor wenigen Jahren wurde jedoch ein möglicher Zusammenhang zwischen erhöhten CRP-Blutplasmawerten und einem erhöhten Risiko für Herz-Kreislauf-Erkrankungen publiziert. Bereits zuvor konnte gezeigt werden, dass erhöhte CRP-Blutplasmawerte nach einem Myokardinfarkt mit einer schlechteren Prognose bezüglich Linksherzinsuffizienz und Tod assoziiert sind. Bis heute konnte jedoch kein kausaler Zusammenhang nachgewiesen werden. Eine elegante Lösung bietet die Dissoziation von pCRP in seine monomeren Untereinheiten (mCRP). mCRP hat proinflammatorische Eigenschaften, die es nicht mit pCRP teilt, wie z.B. C1q Fixation, Thrombozytenaktivierung und Monozytenchemotaxis. Als auslösender Faktor für den Dissoziationsprozess konnten bereits aktivierte Zellmembranen und Liposomen identifiziert werden.

Mikropartikel (MP) sind von Zellen stammende Partikel mit einer Größe zwischen $\sim 0,1$ bis $1 \mu\text{m}$. MP kommen sowohl beim Gesunden als auch beim Kranken im Blutkreislauf vor. Allerdings werden erhöhte Werte von MP vor allem mit inflammatorischen Erkrankungen in Verbindung gebracht. Die genaue Entstehung ist noch nicht endgültig verstanden, aber mehrere Gruppen konnten zeigen, dass steigende zytosolische Calciumlevel nach Zellaktivierung eine Rolle spielen. Die von der Zelle abgegebenen MP repräsentieren in ihrer Membranzusammensetzung anschließend ihre Ursprungszelle. Das bedeutet, dass aktivierte Zellen, bei denen sich die Lipidzusammensetzung der Membranoberfläche geändert hat, diese neue Zusammensetzung an die MP weitergeben. Da sich auch für die Ursprungszelle typische Rezeptoren auf den MP befinden, können diese mit verschiedenen Methoden, wie beispielsweise der Durchflusszytometrie, nachgewiesen werden. So lassen sich MP ihrer

Abstammungszelle zuordnen. Abgesehen von den erhöhten MP Werten können allerdings auch erniedrigte MP Werte mit bestimmten Krankheiten in Verbindung gebracht werden. So sind bei Patienten mit akutem Myokardinfarkt beispielsweise weniger MP in der Blutzirkulation gemessen worden als bei Gesunden. Diese Beobachtung deckte sich mit unseren Ergebnissen.

Der akute Myokardinfarkt (AMI) ist nach wie vor eine der führenden Todesursachen in der westlichen Welt. Alleine 2004 starben in Deutschland beinahe 65000 Patienten an einem Myokardinfarkt oder dessen Folgen. Eine ganze Reihe von Risikofaktoren für die Entstehung der Atherosklerose, der häufigsten Form der koronaren Herzkrankheit welche einen Myokardinfarkt begünstigt, sind über die letzten Jahrzehnte bekannt geworden. Besonders erwähnenswert ist das viel diskutierte CRP, welches seit 2002 mit der Veröffentlichung einer sehr interessanten Studie von Paul Ridker im New England Journal, als möglicher weiterer Risikofaktor betrachtet wird.

Bei der Alzheimer-Krankheit (AK) handelt es sich um die häufigste Form der Demenz. Die Belastung des Patienten, aber auch die der Angehörigen, ist enorm. Es ist daher unbefriedigend, dass keine kausale Therapie existiert. Das liegt zum großen Teil daran, dass der Pathomechanismus, der der AK zu Grunde liegt, nicht hinreichend geklärt ist. Größtenteils ist mittlerweile die These akzeptiert, dass Entzündungsprozesse eine Rolle bei der Entstehung bzw. dem Fortschreiten von Alzheimer spielen. So ist es nicht überraschend, dass das Aktue-Phase-Protein CRP in Senilen Plaques, welche mit der Entstehung der AK in Verbindung stehen, gefunden werden konnte. Auch die Aktivierung des Immunsystems konnte in Hirnschnitten von Patienten mit AK nachgewiesen werden. Ein direkter Zusammenhang zwischen CRP und der AK konnte bis jetzt allerdings nicht gezeigt werden.

Ziele und wissenschaftliche Fragestellung: Diese Doktorarbeit ging der Frage nach, ob MP, welche von aktivierten Zellen stammen, in der Lage sind, genauso wie ihre Ursprungszellen die Dissoziation von pCRP zu mCRP zu triggern und ob die Anti-CRP-Substanz 1,6 Bis-Phosphocholin (BisPC) die Fähigkeit besitzt, diese Dissoziation zu unterbinden. Zudem sollte erstmals der Nachweis von mCRP in der menschlichen Zirkulation erbracht werden.

Darüber hinaus sollte geklärt werden, ob es sich bei dem CRP, welches in Hirnschnitten von Patienten mit der AK gefunden wurde um mCRP handelt. Dies würde womöglich eine Neubewertung von CRP in der AK nach sich ziehen.

Außerdem sollte ein möglicher Auslöser für die Dissoziation von pCRP zu mCRP bei der AK untersucht werden.

Methoden: THP-1 Zellen, HUVEC und humane Blutzellen wurden mit Lipopolysaccharid, TNF- α oder Adenosindiphosphat, respektiv, aktiviert und die entstandenen MP isoliert. Die Zugehörigkeit der isolierten MP zu ihren Ursprungszellen wurde mit der Durchflusszytometrie nachgewiesen. Die Fähigkeit der MP die Dissoziation von pCRP zu mCRP zu initiieren wurde mit nativen Western Blots untersucht. Zudem wurden MP aus Vollblut von Patienten mit AMI sowie einer Kontrollgruppe isoliert und qualitativ mit Western Blot und quantitativ mit Durchflusszytometrie auf mCRP getestet.

Zur Beantwortung der Fragestellungen im Bezug auf die AK wurden Senile Plaques *in vitro* aus Beta-Amyloid 1-42 (A β ₄₂) hergestellt. Die Plaques wurden anschließend mit pCRP inkubiert und mittels Western Blot auf mCRP untersucht. Außerdem wurden die Plaques nach Inkubation mit pCRP in Agarose fixiert, histologisch aufgearbeitet und anschließend mittels Immunhistologie auf mCRP und pCRP gefärbt.

Des Weiteren wurden Hirnschnitte von Patienten mit Alzheimer und von gesunden Kontrollen immunhistologisch auf mCRP gefärbt und quantitativ miteinander verglichen. Zur Evaluation der Assoziation von mCRP mit einer Entzündungsreaktion bei Patienten mit der AK wurden die Hirnschnitte auf Co-Lokalisation von mCRP und C1q sowie mCRP und Senilen Plaques mittels Immunfluoreszenz untersucht.

Ergebnisse: MP von THP-1 Zellen, HUVEC und humanen Blutzellen wurden *in vitro* hergestellt und isoliert. Mit Hilfe von Western Blots konnte gezeigt werden, dass die MP von allen Zelltypen die Dissoziation von pCRP zu mCRP initiieren. Interessanterweise war BisPC, welcher 2 pCRP zu einem Dekamer verbindet, in der Lage diese Dissoziation zu unterbinden. Da mCRP unlöslich ist, konnte es bis jetzt nur *in vitro* und indirekt *in vivo* (immunhistologische Schnitte) nachgewiesen werden. Mit der Isolation von MP von Patienten mit AMI konnte mittels Western Blot und Durchflusszytometrie erstmals mCRP in der Blutzirkulation des Menschen nachgewiesen werden. Außerdem waren signifikant mehr mCRP Banden bei Patienten mit AMI im Vergleich zu einer Kontrollgruppe nachzuweisen ($p < 0,05$). Eine quantitative Erfassung des mCRPs auf den MP erfolgte mit Hilfe der Durchflusszytometrie. Auch hier zeigten die Patienten mit AMI eine signifikant

($p < 0,02$) höhere mittlere Fluoreszenzintensität (525 ± 72) als Patienten der Kontrollgruppe (282 ± 65).

Die Inkubation von A β Plaques mit pCRP zeigte im Western Blot ebenfalls eine Dissoziation des pCRPs zu mCRP. Eine Inkubation von pCRP mit löslichem A β Peptid ohne vorherige Aggregation zu Plaques zeigte diese Eigenschaft hingegen nicht. Auch die immunhistologische Färbung des in Agarose fixierten und mit pCRP inkubierten Plaques zeigte seine Fähigkeit pCRP zu mCRP zu dissoziieren deutlich. In Hirnschnitten von Patienten mit der AK konnte im Vergleich zu gesunden Kontrollen signifikant mehr mCRP nachgewiesen werden ($2,53\% \pm 0,72\%$ vs $0,46\% \pm 0,12\%$; $p < 0.01$). Zudem war in Hirnschnitten von Patienten mit AK hoch signifikant mehr mCRP als pCRP nachzuweisen ($2,53\% \pm 0,72\%$ vs $0,35\% \pm 0,05\%$; $P < 0.01$). Abschließend konnte mithilfe der Immunfluoreszenzdoppelfärbung noch gezeigt werden, dass mCRP co-lokalisiert mit Senilen Plaques und C1q in Hirnschnitten der Patienten zu finden ist.

Diskussion: Diese Arbeit zeigte den ersten Nachweis von mCRP in der menschlichen Zirkulation. Außerdem zeigt diese Arbeit einen möglichen Dissoziationsmechanismus, wie er etwa bei einem AMI vonstattengehen könnte. Interessant ist auch die Erkenntnis, dass signifikant mehr MP mit mCRP in Patienten mit AMI vorhanden sind, als etwa in der Kontrollgruppe. Mit dem Wissen um die proinflammatorischen Eigenschaften des mCRPs sowie der Möglichkeit die Dissoziation mithilfe der Anti-CRP-Substanz BisPC zu unterbinden, stellt sich die Frage, ob die Prognose nach einem AMI mit dem Unterbinden der Dissoziation zu verbessern wäre.

Auch im Zusammenhang mit der AK konnte diese Doktorarbeit neue Erkenntnisse liefern. So handelt es sich bei dem schon vor Jahren nachgewiesenen CRP im Gehirn von Patienten mit der AK um das proinflammatorische mCRP. Als einen möglichen Dissoziationsmechanismus zeigt die Arbeit die Senilen Plaques selbst. Die Co-Lokalisation von mCRP, Senilen Plaques und C1q unterstreicht noch einmal den möglichen Zusammenhang von Entzündung und der AK. Auch hier wird ein neuer therapeutischer Ansatz bei der Behandlung der AK aufgezeigt: Gelingt es die Dissoziation von pCRP zu mCRP durch die Senilen Plaques zu verhindern, könnte unter Umständen der Entzündungsprozess verlangsamt und somit auch das Fortschreiten von Alzheimer reduziert werden.

8 References

1. Pepys MB, Hirschfield GM. (2003) C-reactive protein: a critical update. *J Clin Invest* **111**: 1805-1812.
2. Whitehead AS, Bruns GA, Markham AF, Colten HR, Woods DE. (1983) Isolation of human C-reactive protein complementary DNA and localization of the gene to chromosome 1. *Science* **221**: 69-71.
3. Elliott P, Chambers JC, Zhang W, et al. (2009) Genetic Loci associated with C-reactive protein levels and risk of coronary heart disease. *JAMA* **302**: 37-48.
4. Baltz ML, de Beer FC, Feinstein A, et al. (1982) Phylogenetic aspects of C-reactive protein and related proteins. *Ann N Y Acad Sci* **389**: 49-75.
5. Pepys MB. (2005) CRP or not CRP? That is the question. *Arterioscler Thromb Vasc Biol* **25**: 1091-1094.
6. Suleiman M, Khatib R, Agmon Y, et al. (2006) Early inflammation and risk of long-term development of heart failure and mortality in survivors of acute myocardial infarction predictive role of C-reactive protein. *J Am Coll Cardiol* **47**: 962-968.
7. Pietila KO, Harmoinen AP, Jokiniitty J, Pasternack AI. (1996) Serum C-reactive protein concentration in acute myocardial infarction and its relationship to mortality during 24 months of follow-up in patients under thrombolytic treatment. *Eur Heart J* **17**: 1345-1349.
8. Suleiman M, Aronson D, Reisner SA, et al. (2003) Admission C-reactive protein levels and 30-day mortality in patients with acute myocardial infarction. *Am J Med* **115**: 695-701.
9. Libby P, Ridker PM, Hansson GK. (2009) Inflammation in atherosclerosis: from pathophysiology to practice. *J Am Coll Cardiol* **54**: 2129-2138.
10. Griselli M, Herbert J, Hutchinson WL, et al. (1999) C-reactive protein and complement are important mediators of tissue damage in acute myocardial infarction. *J Exp Med* **190**: 1733-1740.
11. Maier W, Altwegg LA, Corti R, et al. (2005) Inflammatory markers at the site of ruptured plaque in acute myocardial infarction: locally increased interleukin-6 and serum amyloid A but decreased C-reactive protein. *Circulation* **111**: 1355-1361.

12. de Beer FC, Hind CR, Fox KM, Allan RM, Maseri A, Pepys MB. (1982) Measurement of serum C-reactive protein concentration in myocardial ischaemia and infarction. *Br Heart J* **47**: 239-243.
13. Weninger SC, Yankner BA. (2001) Inflammation and Alzheimer disease: the good, the bad, and the ugly. *Nat Med* **7**: 527-528.
14. Akiyama H, Barger S, Barnum S, et al. (2000) Inflammation and Alzheimer's disease. *Neurobiol Aging* **21**: 383-421.
15. Tuppo EE, Arias HR. (2005) The role of inflammation in Alzheimer's disease. *Int J Biochem Cell Biol* **37**: 289-305.
16. Wood JA, Wood PL, Ryan R, et al. (1993) Cytokine indices in Alzheimer's temporal cortex: no changes in mature IL-1 beta or IL-1RA but increases in the associated acute phase proteins IL-6, alpha 2-macroglobulin and C-reactive protein. *Brain Res* **629**: 245-252.
17. Iwamoto N, Nishiyama E, Ohwada J, Arai H. (1994) Demonstration of CRP immunoreactivity in brains of Alzheimer's disease: immunohistochemical study using formic acid pretreatment of tissue sections. *Neurosci Lett* **177**: 23-26.
18. Bottazzi B, Doni A, Garlanda C, Mantovani A. (2010) An integrated view of humoral innate immunity: pentraxins as a paradigm. *Annu Rev Immunol* **28**: 157-183.
19. Hakobyan S, Harris CL, van den Berg CW, et al. (2008) Complement factor H binds to denatured rather than to native pentameric C-reactive protein. *J Biol Chem* **283**: 30451-30460.
20. Koike T, Kitajima S, Yu Y, et al. (2009) Human C-reactive protein does not promote atherosclerosis in transgenic rabbits. *Circulation* **120**: 2088-2094.
21. Kaptoge S, Di Angelantonio E, Lowe G, et al. (2010) C-reactive protein concentration and risk of coronary heart disease, stroke, and mortality: an individual participant meta-analysis. *Lancet* **375**: 132-140.
22. Zacho J, Tybjaerg-Hansen A, Jensen JS, Grande P, Sillesen H, Nordestgaard BG. (2008) Genetically elevated C-reactive protein and ischemic vascular disease. *N Engl J Med* **359**: 1897-1908.
23. Anand SS, Yusuf S. (2010) C-reactive protein is a bystander of cardiovascular disease. *Eur Heart J* **31**: 2092-2096.

24. Eisenhardt SU, Habersberger J, Murphy A, et al. (2009) Dissociation of pentameric to monomeric C-reactive protein on activated platelets localizes inflammation to atherosclerotic plaques. *Circ Res* **105**: 128-137.
25. Ji SR, Wu Y, Zhu L, et al. (2007) Cell membranes and liposomes dissociate C-reactive protein (CRP) to form a new, biologically active structural intermediate: mCRP(m). *FASEB J* **21**: 284-294.
26. Molins B, Pena E, Vilahur G, Mendieta C, Slevin M, Badimon L. (2008) C-reactive protein isoforms differ in their effects on thrombus growth. *Arterioscler Thromb Vasc Biol* **28**: 2239-2246.
27. Pisetsky DS. (2009) Microparticles as biomarkers in autoimmunity: from dust bin to center stage. *Arthritis Res Ther* **11**: 135.
28. Hugel B, Martinez MC, Kunzelmann C, Freyssinet JM. (2005) Membrane microparticles: two sides of the coin. *Physiology (Bethesda)* **20**: 22-27.
29. Thery C, Zitvogel L, Amigorena S. (2002) Exosomes: composition, biogenesis and function. *Nat Rev Immunol* **2**: 569-579.
30. Martinez MC, Tesse A, Zobairi F, Andriantsitohaina R. (2005) Shed membrane microparticles from circulating and vascular cells in regulating vascular function. *Am J Physiol Heart Circ Physiol* **288**: H1004-1009.
31. Boulanger CM, Amabile N, Tedgui A. (2006) Circulating microparticles: a potential prognostic marker for atherosclerotic vascular disease. *Hypertension* **48**: 180-186.
32. Messer L, Alsaleh G, Freyssinet JM, et al. (2009) Microparticle-induced release of B-lymphocyte regulators by rheumatoid synoviocytes. *Arthritis Res Ther* **11**: R40.
33. MacKenzie A, Wilson HL, Kiss-Toth E, Dower SK, North RA, Surprenant A. (2001) Rapid secretion of interleukin-1beta by microvesicle shedding. *Immunity* **15**: 825-835.
34. Nomura S, Tandon NN, Nakamura T, Cone J, Fukuhara S, Kambayashi J. (2001) High-shear-stress-induced activation of platelets and microparticles enhances expression of cell adhesion molecules in THP-1 and endothelial cells. *Atherosclerosis* **158**: 277-287.
35. Leroyer AS, Tedgui A, Boulanger CM. (2008) Role of microparticles in atherothrombosis. *J Intern Med* **263**: 528-537.

36. Miyazaki Y, Nomura S, Miyake T, et al. (1996) High shear stress can initiate both platelet aggregation and shedding of procoagulant containing microparticles. *Blood* **88**: 3456-3464.
37. Miyoshi H, Umeshita K, Sakon M, et al. (1996) Calpain activation in plasma membrane bleb formation during tert-butyl hydroperoxide-induced rat hepatocyte injury. *Gastroenterology* **110**: 1897-1904.
38. Wiedmer T, Sims PJ. (1991) Participation of protein kinases in complement C5b-9-induced shedding of platelet plasma membrane vesicles. *Blood* **78**: 2880-2886.
39. Combes V, Simon AC, Grau GE, et al. (1999) In vitro generation of endothelial microparticles and possible prothrombotic activity in patients with lupus anticoagulant. *J Clin Invest* **104**: 93-102.
40. Fox JE, Austin CD, Reynolds CC, Steffen PK. (1991) Evidence that agonist-induced activation of calpain causes the shedding of procoagulant-containing microvesicles from the membrane of aggregating platelets. *J Biol Chem* **266**: 13289-13295.
41. Fox JE, Austin CD, Boyles JK, Steffen PK. (1990) Role of the membrane skeleton in preventing the shedding of procoagulant-rich microvesicles from the platelet plasma membrane. *J Cell Biol* **111**: 483-493.
42. Enjeti AK, Lincz LF, Seldon M. (2008) Microparticles in health and disease. *Semin Thromb Hemost* **34**: 683-691.
43. Op den Kamp JA. (1979) Lipid asymmetry in membranes. *Annu Rev Biochem* **48**: 47-71.
44. Gilbert GE, Sims PJ, Wiedmer T, Furie B, Furie BC, Shattil SJ. (1991) Platelet-derived microparticles express high affinity receptors for factor VIII. *J Biol Chem* **266**: 17261-17268.
45. Sims PJ, Faioni EM, Wiedmer T, Shattil SJ. (1988) Complement proteins C5b-9 cause release of membrane vesicles from the platelet surface that are enriched in the membrane receptor for coagulation factor Va and express prothrombinase activity. *J Biol Chem* **263**: 18205-18212.
46. Hamilton KK, Hattori R, Esmon CT, Sims PJ. (1990) Complement proteins C5b-9 induce vesiculation of the endothelial plasma membrane and expose catalytic surface for assembly of the prothrombinase enzyme complex. *J Biol Chem* **265**: 3809-3814.

47. Hoffman M, Monroe DM, Roberts HR. (1992) Coagulation factor IXa binding to activated platelets and platelet-derived microparticles: a flow cytometric study. *Thromb Haemost* **68**: 74-78.
48. Castaman G, Yu-Feng L, Battistin E, Rodeghiero F. (1997) Characterization of a novel bleeding disorder with isolated prolonged bleeding time and deficiency of platelet microvesicle generation. *Br J Haematol* **96**: 458-463.
49. Maly M, Hrachovinova I, Tomasov P, Salaj P, Hajek P, Veselka J. (2009) Patients with acute coronary syndromes have low tissue factor activity and microparticle count, but normal concentration of tissue factor antigen in platelet free plasma: a pilot study. *Eur J Haematol* **82**: 148-153.
50. WHO. (2008) The top 10 causes of death. The World Health Organisation.
51. Smith SC, Jr., Allen J, Blair SN, et al. (2006) AHA/ACC guidelines for secondary prevention for patients with coronary and other atherosclerotic vascular disease: 2006 update: endorsed by the National Heart, Lung, and Blood Institute. *Circulation* **113**: 2363-2372.
52. Buse JB, Ginsberg HN, Bakris GL, et al. (2007) Primary prevention of cardiovascular diseases in people with diabetes mellitus: a scientific statement from the American Heart Association and the American Diabetes Association. *Circulation* **115**: 114-126.
53. Graham I, Atar D, Borch-Johnsen K, et al. (2007) European guidelines on cardiovascular disease prevention in clinical practice: executive summary: Fourth Joint Task Force of the European Society of Cardiology and Other Societies on Cardiovascular Disease Prevention in Clinical Practice (Constituted by representatives of nine societies and by invited experts). *Eur Heart J* **28**: 2375-2414.
54. Yusuf S, Hawken S, Ounpuu S, et al. (2005) Obesity and the risk of myocardial infarction in 27,000 participants from 52 countries: a case-control study. *Lancet* **366**: 1640-1649.
55. Ridker PM, Rifai N, Rose L, Buring JE, Cook NR. (2002) Comparison of C-reactive protein and low-density lipoprotein cholesterol levels in the prediction of first cardiovascular events. *N Engl J Med* **347**: 1557-1565.
56. Alpert JS, Thygesen K, Antman E, Bassand JP. (2000) Myocardial infarction redefined--a consensus document of The Joint European Society of Cardiology/American College of Cardiology Committee for the redefinition of myocardial infarction. *J Am Coll Cardiol* **36**: 959-969.

57. Hendrie HC. (1998) Epidemiology of dementia and Alzheimer's disease. *Am J Geriatr Psychiatry* **6**: S3-18.
58. Alzheimer. (1907) Über eine eigenartige Erkrankung der Hirnrinde. *Allgemeine Zeitschrift für Psychiatrie und Psychisch-Gerichtliche Medizin* **64**: 146-148.
59. Ferri CP, Prince M, Brayne C, et al. (2005) Global prevalence of dementia: a Delphi consensus study. *Lancet* **366**: 2112-2117.
60. Selkoe DJ. (2001) Alzheimer's disease: genes, proteins, and therapy. *Physiol Rev* **81**: 741-766.
61. Mahley RW, Weisgraber KH, Huang Y. (2006) Apolipoprotein E4: a causative factor and therapeutic target in neuropathology, including Alzheimer's disease. *Proc Natl Acad Sci U S A* **103**: 5644-5651.
62. Corder EH, Saunders AM, Strittmatter WJ, et al. (1993) Gene dose of apolipoprotein E type 4 allele and the risk of Alzheimer's disease in late onset families. *Science* **261**: 921-923.
63. Strittmatter WJ, Saunders AM, Schmechel D, et al. (1993) Apolipoprotein E: high-avidity binding to beta-amyloid and increased frequency of type 4 allele in late-onset familial Alzheimer disease. *Proc Natl Acad Sci U S A* **90**: 1977-1981.
64. Polvikoski T, Sulkava R, Haltia M, et al. (1995) Apolipoprotein E, dementia, and cortical deposition of beta-amyloid protein. *N Engl J Med* **333**: 1242-1247.
65. Walsh DM, Selkoe DJ. (2007) A beta oligomers - a decade of discovery. *J Neurochem* **101**: 1172-1184.
66. Mudher A, Lovestone S. (2002) Alzheimer's disease-do tauists and baptists finally shake hands? *Trends Neurosci* **25**: 22-26.
67. Goedert M, Spillantini MG, Crowther RA. (1991) Tau proteins and neurofibrillary degeneration. *Brain Pathol* **1**: 279-286.
68. Citron M. (2010) Alzheimer's disease: strategies for disease modification. *Nat Rev Drug Discov* **9**: 387-398.
69. Selkoe DJ. (1999) Translating cell biology into therapeutic advances in Alzheimer's disease. *Nature* **399**: A23-31.
70. Rogers J, Cooper NR, Webster S, et al. (1992) Complement activation by beta-amyloid in Alzheimer disease. *Proc Natl Acad Sci U S A* **89**: 10016-10020.

71. Akiyama H, Arai T, Kondo H, Tanno E, Haga C, Ikeda K. (2000) Cell mediators of inflammation in the Alzheimer disease brain. *Alzheimer Dis Assoc Disord* **14 Suppl 1**: S47-53.
72. Paravastu AK, Petkova AT, Tycko R. (2006) Polymorphic fibril formation by residues 10-40 of the Alzheimer's beta-amyloid peptide. *Biophys J* **90**: 4618-4629.
73. Kresl JJ, Potempa LA, Anderson BE. (1998) Conversion of native oligomeric to a modified monomeric form of human C-reactive protein. *Int J Biochem Cell Biol* **30**: 1415-1426.
74. Brodsky SV, Malinowski K, Golightly M, Jesty J, Goligorsky MS. (2002) Plasminogen activator inhibitor-1 promotes formation of endothelial microparticles with procoagulant potential. *Circulation* **106**: 2372-2378.
75. Waldvogel HJ, Curtis MA, Baer K, Rees MI, Faull RL. (2006) Immunohistochemical staining of post-mortem adult human brain sections. *Nat Protoc* **1**: 2719-2732.
76. Slevin M, Matou-Nasri S, Turu M, et al. (2010) Modified C-reactive protein is expressed by stroke neovessels and is a potent activator of angiogenesis in vitro. *Brain Pathol* **20**: 151-165.
77. Yang L, Froio RM, Sciuto TE, Dvorak AM, Alon R, Luscinskas FW. (2005) ICAM-1 regulates neutrophil adhesion and transcellular migration of TNF-alpha-activated vascular endothelium under flow. *Blood* **106**: 584-592.
78. Pepys MB, Hirschfield GM, Tennent GA, et al. (2006) Targeting C-reactive protein for the treatment of cardiovascular disease. *Nature* **440**: 1217-1221.
79. Slevin M, Matou-Nasri S, Turu M, et al. (2009) Modified C-reactive protein is expressed by stroke neovessels and is a potent activator of angiogenesis in vitro. *Brain Pathol* **20**: 151-165.
80. Herczenik E, Bouma B, Korporaal SJ, et al. (2007) Activation of human platelets by misfolded proteins. *Arterioscler Thromb Vasc Biol* **27**: 1657-1665.
81. Kowalska MA, Badellino K. (1994) beta-Amyloid protein induces platelet aggregation and supports platelet adhesion. *Biochem Biophys Res Commun* **205**: 1829-1835.
82. Fiala M, Zhang L, Gan X, et al. (1998) Amyloid-beta induces chemokine secretion and monocyte migration across a human blood-brain barrier model. *Mol Med* **4**: 480-489.

83. Eisenhardt SU, Habersberger J, Oliva K, et al. (2011) A proteomic analysis of C-reactive protein stimulated THP-1 monocytes. *Proteome Sci* **9**: 1.
84. van der Zee PM, Biro E, Trouw LA, et al. (2010) C-reactive protein in myocardial infarction binds to circulating microparticles but is not associated with complement activation. *Clin Immunol* **135**: 490-495.
85. Torzewski M, Rist C, Mortensen RF, et al. (2000) C-reactive protein in the arterial intima: role of C-reactive protein receptor-dependent monocyte recruitment in atherogenesis. *Arterioscler Thromb Vasc Biol* **20**: 2094-2099.
86. Lagrand WK, Niessen HW, Wolbink GJ, et al. (1997) C-reactive protein colocalizes with complement in human hearts during acute myocardial infarction. *Circulation* **95**: 97-103.
87. Bisoendial RJ, Boekholdt SM, Vergeer M, Stroes ES, Kastelein JJ. (2010) C-reactive protein is a mediator of cardiovascular disease. *Eur Heart J* **31**: 2087-2091.
88. Anzai T, Yoshikawa T, Shiraki H, et al. (1997) C-reactive protein as a predictor of infarct expansion and cardiac rupture after a first Q-wave acute myocardial infarction. *Circulation* **96**: 778-784.
89. Potempa LA, Maldonado BA, Laurent P, Zemel ES, Gewurz H. (1983) Antigenic, electrophoretic and binding alterations of human C-reactive protein modified selectively in the absence of calcium. *Mol Immunol* **20**: 1165-1175.
90. Casas JP, Shah T, Hingorani AD, Danesh J, Pepys MB. (2008) C-reactive protein and coronary heart disease: a critical review. *J Intern Med* **264**: 295-314.
91. Sjowall C, Bengtsson AA, Sturfelt G, Skogh T. (2004) Serum levels of autoantibodies against monomeric C-reactive protein are correlated with disease activity in systemic lupus erythematosus. *Arthritis Res Ther* **6**: R87-94.
92. Tan Y, Yu F, Qu Z, et al. (2011) Modified C-reactive protein might be a target autoantigen of TINU syndrome. *Clin J Am Soc Nephrol* **6**: 93-100.
93. Strang F, Scheichl A, Chen YC, et al. (2012) Amyloid plaques dissociate pentameric to monomeric C-reactive protein: a novel pathomechanism driving cortical inflammation in Alzheimer's disease? *Brain Pathol* **22**: 337-346.

94. Zwaal RF, Schroit AJ. (1997) Pathophysiologic implications of membrane phospholipid asymmetry in blood cells. *Blood* **89**: 1121-1132.
95. Rhodes B, Furnrohr BG, Vyse TJ. (2011) C-reactive protein in rheumatology: biology and genetics. *Nat Rev Rheumatol* **7**: 282-289.
96. Biro A, Rovo Z, Papp D, et al. (2007) Studies on the interactions between C-reactive protein and complement proteins. *Immunology* **121**: 40-50.
97. Majka M, Kijowski J, Lesko E, Gozdzik J, Zupanska B, Ratajczak MZ. (2007) Evidence that platelet-derived microvesicles may transfer platelet-specific immunoreactive antigens to the surface of endothelial cells and CD34+ hematopoietic stem/ progenitor cells--implication for the pathogenesis of immune thrombocytopenias. *Folia Histochem Cytobiol* **45**: 27-32.
98. Boilard E, Nigrovic PA, Larabee K, et al. (2010) Platelets amplify inflammation in arthritis via collagen-dependent microparticle production. *Science* **327**: 580-583.
99. Eisenhardt SU, Habersberger J, Peter K. (2009) Monomeric C-reactive protein generation on activated platelets: the missing link between inflammation and atherothrombotic risk. *Trends Cardiovasc Med* **19**: 232-237.
100. Wang MS, Black JC, Knowles MK, Reed SM. (2011) C-reactive protein (CRP) aptamer binds to monomeric but not pentameric form of CRP. *Anal Bioanal Chem* **401**: 1309-1318.
101. Yasojima K, Schwab C, McGeer EG, McGeer PL. (2000) Human neurons generate C-reactive protein and amyloid P: upregulation in Alzheimer's disease. *Brain Res* **887**: 80-89.
102. Duong T, Nikolaeva M, Acton PJ. (1997) C-reactive protein-like immunoreactivity in the neurofibrillary tangles of Alzheimer's disease. *Brain Res* **749**: 152-156.
103. Yasojima K, Schwab C, McGeer EG, McGeer PL. (2001) Generation of C-reactive protein and complement components in atherosclerotic plaques. *Am J Pathol* **158**: 1039-1051.
104. Stolp HB, Dziegielewska KM. (2009) Review: Role of developmental inflammation and blood-brain barrier dysfunction in neurodevelopmental and neurodegenerative diseases. *Neuropathol Appl Neurobiol* **35**: 132-146.

105. Dimopoulos N, Piperi C, Salonicioti A, et al. (2006) Indices of low-grade chronic inflammation correlate with early cognitive deterioration in an elderly Greek population. *Neurosci Lett* **398**: 118-123.
106. Gupta A, Watkins A, Thomas P, et al. (2005) Coagulation and inflammatory markers in Alzheimer's and vascular dementia. *Int J Clin Pract* **59**: 52-57.
107. Zaciragic A, Lepara O, Valjevac A, et al. (2007) Elevated serum C-reactive protein concentration in Bosnian patients with probable Alzheimer's disease. *J Alzheimers Dis* **12**: 151-156.
108. Xu G, Zhou Z, Zhu W, Fan X, Liu X. (2009) Plasma C-reactive protein is related to cognitive deterioration and dementia in patients with mild cognitive impairment. *J Neurol Sci* **284**: 77-80.
109. Ciubotaru I, Potempa LA, Wander RC. (2005) Production of modified C-reactive protein in U937-derived macrophages. *Exp Biol Med (Maywood)* **230**: 762-770.
110. Potempa LA, Siegel JN, Fiedel BA, Potempa RT, Gewurz H. (1987) Expression, detection and assay of a neoantigen (Neo-CRP) associated with a free, human C-reactive protein subunit. *Mol Immunol* **24**: 531-541.
111. Makinen S, van Groen T, Clarke J, et al. (2008) Coaccumulation of calcium and beta-amyloid in the thalamus after transient middle cerebral artery occlusion in rats. *J Cereb Blood Flow Metab* **28**: 263-268.
112. Lin HB, Yang XM, Li TJ, Cheng YF, Zhang HT, Xu JP. (2009) Memory deficits and neurochemical changes induced by C-reactive protein in rats: implication in Alzheimer's disease. *Psychopharmacology (Berl)* **204**: 705-714.
113. Veerhuis R. (2011) Histological and direct evidence for the role of complement in the neuroinflammation of AD. *Curr Alzheimer Res* **8**: 34-58.
114. Ji SR, Wu Y, Potempa LA, Liang YH, Zhao J. (2006) Effect of modified C-reactive protein on complement activation: a possible complement regulatory role of modified or monomeric C-reactive protein in atherosclerotic lesions. *Arterioscler Thromb Vasc Biol* **26**: 935-941.
115. Morganti-Kossmann MC, Rancan M, Otto VI, Stahel PF, Kossmann T. (2001) Role of cerebral inflammation after traumatic brain injury: a revisited concept. *Shock* **16**: 165-177.

116. Gill R, Kemp JA, Sabin C, Pepys MB. (2004) Human C-reactive protein increases cerebral infarct size after middle cerebral artery occlusion in adult rats. *J Cereb Blood Flow Metab* **24**: 1214-1218.

9 Acknowledgement

I would like to thank Prof. Dr. Peter from the Baker IDI Heart and Diabetes Institute in Melbourne, Australia for providing me with a working place in his laboratory, for his support and his help with finding new approaches to difficult questions.

Then I would like to thank Prof. Dr. Schunkert from the UKSH, Campus Lübeck for his generous support in writing this thesis and his support in giving me the chance to do most of my work abroad.

Moreover I thank Nicole Bassler for her help with technical approaches, for teaching me methods and being patience with me learning these methods.

A very big thank to Dr. Habersberger, the best colleague you can wish for, who was always happy to discuss results, who was always helpful with methods, questions, approaches and/or writing manuscripts. I can't say thanks enough.

Another thanks goes to my newer colleague Amelie Scheichl for working that hard on this project with me.

At last I would like to thank my parents as I wouldn't have been able to do what I did without their incredible support in everything, really everything.

10 Curriculum Vita

Persönliche Angaben

Name	Frederik Strang
Geburtsdatum	02.02.1984
Geburtsort	Eckernförde
Familienstand	ledig
Staatsangehörigkeit	deutsch



Studium und Förderungen

04/2006 – 04/2008	Medizinstudium an der Universität Göttingen 1. Abschnitt der ärztlichen Prüfung: 3,0
04/2008 – 10/2012	Medizinstudium an der Universität zu Lübeck 2. Abschnitt der ärztlichen Prüfung: 2,0
02/2010 – 10/2010	Praktischer Teil meiner Dissertation am Baker IDI in Melbourne, Australien
07/2010 – 06/2011	Stipendium „Exzellenzmedizin“ der Universität zu Lübeck
10/2010	Förderung des Auslandsaufenthaltes im Rahmen des PROMOS Programms des DAAD

Famulaturen

07/2008	4 Wochen in der kardiologischen Praxis Dr. Keutel in Lübeck
02/2009	4 Wochen in der Kardiologie im Alfred Hospital in Melbourne
08/2009	3 Wochen Orthopädie an der Universität zu Lübeck
09/2009	2 Wochen Kardiologie am Herzzentrum in Bad Segeberg
02/2011	3 Wochen Kardiologie am Tygerberg Academic Hospital in Kapstadt

Praktisches Jahr

1. Tertial (Innere Medizin)	4 Wochen interdisziplinäre Notaufnahme des UKSH, Lübeck 4 Wochen Rhythmologie, UKSH, Campus Lübeck 8 Wochen interdisziplinäre Intensivstation UKSH, Lübeck
2. Tertial (Anästhesie)	8 Wochen am Spital Limmattal, Schweiz 8 Wochen am Sana Klinikum Lübeck, davon 4 Wo. Intensivst.
3. Tertial (Chirurgie)	12 Wochen an der Schön Klinik Neustadt, davon 3 Wochen Notaufnahme

11 Publications

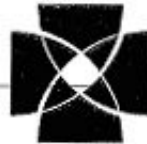
Parts of this thesis have already been published (chronological order):

1. Oral presentation with the title “Circulating microparticles dissociate pentameric to monomeric C-reactive protein in patients with acute myocardial infarction” at the annual scientific meeting of The Australian Vascular Biology Society 2010 in Lorne. **Winner of the first prize** in the student’s category for an outstanding presentation.
2. Habersberger J, **Strang F**, Eisenhardt SU, Du, X-J, Peter K. Monomeric CRP is generated in patients following myocardial infarction and is deposited in infarcted tissue; a pathomechanistic link between CRP and necrosis. *Poster at the European Society of Cardiology meeting 2011* in Paris.
3. **Strang F**, Scheichl A, Chen YC, Wang X, Htun NM, Bassler N, Eisenhardt S, Habersberger J, Peter K. Amyloid plaques dissociate pentameric to monomeric C-Reactive-Protein: A novel pathomechanism driving cortical inflammation in Alzheimer's disease? *Brain Pathol.* 2012 May 22.
4. Habersberger J*, **Strang F***, Scheichl A,* Htun N, Bassler N, Merivita RM, Diehl P, Krippner G, Meikle P, Eisenhardt SU, Meredith I, Peter K. Circulating microparticles generate and transport monomeric C-reactive protein in patients with acute myocardial infarction. *CVR* 2012 July 13.

* equally contributing first authors

12 Attachments

12.1 Ethics approval for mCRP detection after myocard infarction



TheAlfred

Ethics Committee

Certificate of Approval of Amendments

This is to certify that amendments to

**Project 189/06 Detection of different C-reactive protein conformations
involved in acute coronary syndrome**

Principal Researchers: Dr Steffen Eisenhardt & Professor Karlheinz Peter

Amendment:

**Changes to research personnel (departure of Ruide Koh & Chen Sheng; addition
of Dr Jonathon Habersberger);
decrease in participant numbers (from 40 to 20);
addition of 2nd blood sample for some participants; changes to sample
preparation;
revised Module One, revised Module Three
Participant Information & Consent Form Version 6 dated: 08-Apr-2010**

have been approved in accordance with your amendment application dated
17-Apr-2010 on the understanding that you observe the National Statement on
Ethical Conduct in Human Research.

It is now your responsibility to ensure that all people associated with this
particular research project are made aware of what has actually been approved
and any caveats specified in correspondence with the Ethics Committee. Any
further change to the application which is likely to have a significant impact on
the ethical considerations of this project will require approval from the Ethics
Committee.

Chair, Ethics Committee (or delegate)

Date: 28-Apr-2010

**R. FREW
SECRETARY
ETHICS COMMITTEE**

*All research subject to Alfred Hospital Ethics Committee review must be conducted in accordance with
the National Statement on Ethical Conduct in Human Research (2007).*

*The Alfred Ethics Committee is a properly constituted Human Research Ethics Committee operating in
accordance with the National Statement on Ethical Conduct in Human Research (2007).*

AMREP ANIMAL ETHICS COMMITTEE



MEMORANDUM

TO: Jonathon Habersberger

FROM: AEC Secretary – Leia Demtschyna

DATE: Monday, 07 December 2009

SUBJECT: AEC APPLICATION 1902 – APPROVAL

Dear Jonathon,

The AMREP Animal Ethics Committee has considered and approved your application:

Establishing monomeric C reactive protein as a		APPROVAL	
TITLE: pathological agent in myocardial infarction.		DATE: 07/12/2009	
SPECIES/STRAIN:	Rat/SD o/b	NO. OF ANIMALS APPROVED:	90
APPLICATION NO.	1902	Closure Date: 15/06/2012	
AEC APPROVED PROJECT NUMBER:		E/0899/2009/B	
SCIENTIFIC LICENCE: Baker IDI and Diabetes institute			

Obtaining Animals: All requests for animals and services related to this project must be made through the Precinct Animal Centre. Advanced planning will assist the PAC in supplying animals and services. Animals requiring special housing conditions, e.g. PC2, must be clearly identified on your orders.

Facility Use: Use of animals in this project must be in compliance with the Australian Code of Practice for the care and use of animals for scientific purposes, 7th edition and BMRI Policy and Guidelines. Introduction of new colonies and species need to be applied for through the AMREPAEC Committee.

OH&S Issues: As the responsible investigator please ensure that all personnel who may be exposed to potentially biohazardous material are informed of any risks and how best to avoid them. This includes notifying PAC management of such issues.

Reports: You are required to complete an annual progress report on this application for the AEC committee. On completion of the project you are required to submit to the AEC a final report. You are required to complete an annual report for the Bureau of Animal Welfare. You are required to maintain experimental records as defined in the Australian Code of Practice for the care and use of animals for scientific purposes, 7th edition. These records must be made available when requested.

The AEC may undertake an inspection or ask for a progress report at any time during this project.

Yours sincerely,

AMREP AEC SECRETARY
On Behalf of the AMREP AEC

12.2 Ethics approval for mCRP detection in Alzheimer patient's brain tissue



TheAlfred

ETHICS COMMITTEE CERTIFICATE OF APPROVAL

This is to certify that

Project No: 150/10

Project Title: Detection of mCRP in senile plaques formed by beta amyloid protien in alzheimer's disease patient's brain tissue

Principal Researcher: Prof Peter Karlheinz

*was considered for Low Risk Review and **APPROVED** on 06-May-2010*

It is the Principal Researcher's responsibility to ensure that all researchers associated with this project are aware of the conditions of approval and which documents have been approved.

The Principal Researcher is required to notify the Secretary of the Ethics Committee, via amendment or progress report, of

- Any significant change to the project and the reason for that change, including an indication of ethical implications (if any);
- Serious adverse effects on participants and the action taken to address those effects;
- Any other unforeseen events or unexpected developments that merit notification;
- The inability of the Principal Researcher to continue in that role, or any other change in research personnel involved in the project;
- A delay of more than 12 months in the commencement of the project; and,
- Termination or closure of the project.

Additionally, the Principal Researcher is required to submit

- A Progress Report on the anniversary of approval and on completion of the project .

Approval covers the project as described in the application (including any modifications made prior to approval). Low Risk projects are subject to audit and ethical approval may be withdrawn if the project deviates from that proposed and approved.

SPECIAL CONDITIONS

None

SIGNED: 
Chair, Ethics Committee (or delegate)

**R. FREW
SECRETARY
ETHICS COMMITTEE**

Please quote Project No and Title in all correspondence